Optimal Sensor Threshold Control and the Weapon Operating Characteristic for Autonomous Search and Attack Munitions

THESIS

Roland A. Rosario, Captain, USAF

AFIT/GAE/ENG/07-02

DEPARTMENT OF THE AIR FORCE
AIR UNIVERSITY

AIR FORCE INSTITUTE OF TECHNOLOGY

Wright-Patterson Air Force Base, Ohio

The views expressed in this thesis are those of the author and do not reflect the official policy or position of the United States Air Force, Department of Defense, or the United States Government.

AFIT/GAE/ENG/07-02

Optimal Sensor Threshold Control and the Weapon Operating Characteristic for Autonomous Search and Attack Munitions

THESIS

Presented to the Faculty

Department of Electrical and Computer Engineering

Graduate School of Engineering and Management

Air Force Institute of Technology

Air University

Air Education and Training Command

In Partial Fulfillment of the Requirements for the

Degree of Master of Science in Aeronautical Engineering

Roland A. Rosario, B.S.

Captain, USAF

March 2007

AFIT/GAE/ENG/07-02

Optimal Sensor Threshold Control and the Weapon Operating Characteristic for Autonomous Search and Attack Munitions

Roland A. Rosario, B.S.
Captain, USAF

Approved:

/signed/	7 Mar 2007
Dr. Meir Pachter (Chairman)	date
/signed/	7 Mar 2007
Dr. David Jacques (Member)	date
/signed/	7 Mar 2007
Maj Paul Blue (Member)	date

AFIT/GAE/ENG/07-02

Abstract

This thesis considers the optimal employment of a wide area search munition in a battlespace where a target is known to be uniformly distributed among false targets which are Poisson distributed. The Poisson distribution's parameter is obtained from readily available battlespace intelligence. This work formulates and solves the optimal control problem for deriving the optimal sensor threshold schedule in order to maximize the probability of attacking the target during the battlespace sweep while constraining the probability of attacking a false target. The efficiency gained by optimally varying the sensor threshold is compared against the performance achieved with a static, optimum sensor threshold setting. The Weapon Operating Characteristic, the relationship between maximum achievable probability of target attack and maximum allowable probability of false target attack, is developed.

Acknowledgements

Thank you, Dr. Pachter, for teaching me. Bright, patient, sagacious and humble, you are the ideal instructor. My thesis journey has been very fruitful. Thank you as well to Dr. Jacques and Maj Blue, the other two members of my thesis committee, for your continued support and educational insight during this process.

Roland A. Rosario

Table of Contents

Page

List of Figures

List of Tables

List of Symbols

Symbol		Page
P_k	Probability of Kill	5
P_{TA}	Probability of attacking the desired target	14
P_{FTA}	Probability of false target attack	14
v	Munition velocity	17
w	Munition's sensor swath width	17
A	Area (km^2)	17
t	time (sec)	18
A_s	Total battlespace search area (km^2)	18
T	Total battlespace search duration (sec)	18
α	False target density	19
L	Number of false targets in the battlespace search area	19
$P_{\overline{FTA}}$	Probability of not attacking a false target	20
P_{TR}	Probability of target report	22
P_{FTR}	Probability of false target report	22
c	ROC parameter	24
λ_{FT}	Poisson parameter for false targets	31

List of Abbreviations

Abbreviation		Page
UAVs	Unmanned Aerial Vehicles	1
AFIT	Air Force Institute of Technology	2
CONOPS	Concept of Operations	4
ROE	Rules of Engagement	4
WASM	Wide Area Search Munition	5
ATR	Automatic Target Recognition	5
WOC	WASM Operating Characteristic	6
RSM	Response Surface Methodology	13
FT	False Target	17
ROC	Receiver Operating Characteristic	24
pdf	probability density function	29
AFRL	Air Force Research Laboratory	65

Optimal Sensor Threshold Control and the Weapon Operating Characteristic for Autonomous Search and Attack Munitions

I. Introduction

1.1 Overview

Ever increasing technological advancements have substantially contributed to autonomous technology. In particular, the aerospace industry has seen increased research and development efforts towards autonomous unmanned aerial vehicles (UAVs). Currently, UAVs perform a wide range of wartime (and peacetime) activities including reconnaissance, and in some cases, attack. The spectrum of UAVs includes high-value assets, akin to modern, multi-role aerial platforms, to inexpensive, disposable platforms designed to execute a single mission or task. The new capability afforded by these autonomous assets fills an important role in new emerging paradigms characteristic of the Western style of war. One persistent, almost dogmatic, theme has been to "do more with less". This concept is supported by the emergence of better autonomous technology because, in many cases, UAVs and other forms of autonomous technology are able to automate and perform tasks that otherwise require intensive commitment of human and other resources. Furthermore, autonomous machines are not as limited as humans in the bandwidth of cooperation. Because of the benefits to be gained by cooperative synergism, cooperative control of autonomous agents, enabled by improvements in modern, autonomous systems, is in parallel development with autonomous machines.

This research addresses optimal control algorithms for UAVs autonomously performing search and destroy missions. Cooperative control could be further applied to optimize the performance of a swarm of autonomous munitions; however, it is desirable to have each individual agent acting autonomously before implementing co-

operative capabilities. The optimal control aspect is the focus of this thesis, namely, the performance optimization of individual autonomous agents. This research follows previous work done (mostly at the Air Force Institute of Technology—AFIT) in similar areas. Specifically, this thesis investigates the mission efficiency to be gained from optimal control of dynamically varying parameters such as the agent's sensor threshold. This chapter will be followed by a detailed mathematical buildup and discussion of the previous work that has been accomplished in this area and then by the actual methodology and results on this research. The rest of this chapter will address the scope, motivation, historical background, objectives and a concise summary of this research.

1.2 Scope

Cooperative control is a relatively new discipline that covers a wide range of topics dealing with establishing a scheme of cooperation among autonomous agents. In other words, cooperative control efforts attempt to network and integrate machines so they can work together to achieve greater utility as defined by their objectives, much in the same way as humans inherently act in a group sharing the same goal. Cooperative control includes such topics as formation flight, path planning and automated aerial refueling. The objective of these examples is to increase the efficiency of the mission by synergizing the efforts of the involved agents. For instance, consider cooperative path planning of autonomous UAVs. The optimal path for a single vehicle given a set of objectives is readily derived. Cooperative path planning seeks to reconfigure that trajectory to incorporate awareness of other vehicles. A cooperative path plan will incorporate multiple assets into the overall mission by positioning each vehicle to maximize the overall objective success, not necessarily with respect to one vehicle or another. In most cases, the overall mission efficiency of a cooperative mission is greater than can be achieved by a single asset.

The subset of cooperative control that this research addresses is cooperative search, classification, and attack. As the name would suggest, the aim is to configure

agents, each with the individual capability to autonomously search for targets, classify them as true or false targets, and decide to attack them with awareness of other munitions in the same area trying to achieve the same goal. This thesis is further scoped to address the optimization of an individual munition's performance. Previous work has already shown that substantial mission efficiency may be gained by cooperatively controlling a swarm of such autonomous munitions in an area as opposed to releasing individual munitions in an area each with the individual search, classification and attack objective, but lacking awareness of the other collocated agents. In the future, the previous work on cooperative decision making should be combined with the results of this thesis, namely, the optimal sensor threshold control of autonomous munitions, to achieve increased performance from an autonomous swarm. Obviously this scenario is futuristic—one in which policy makers and the general public trust and rely upon autonomous machines to safely and effectively perform lethal, wartime missions. However, garnering support and engendering confidence in this budding theory is one of the advantages of this research.

1.3 Motivation

There are ample potential benefits of this research. First, this thesis supports the paradigm shift introduced above—that modern approaches to conducting warfare increasingly seek methods of doing more with less. The most valued resource in military operations is the human resource. When able, it is desirable to decrease the risk to human beings as much as possible. To this end, it is desirable to use autonomous agents for as many tasks as possible, the prospect of which is becoming more and more feasible with advances in technology. At the same time that use of autonomous machines mitigates the risk to humans in hazardous environments, cooperative control of said machines is useful for increasing the overall mission efficiency. For the same reason that many human-performed, combat air operations are carried out in flights of aircraft instead of individual aircraft, cooperative control of machines carrying the

same tasks may result in increased mission efficiency. Several examples of this shown in previous research are presented in chapter II of this thesis.

Another motivating factor of this research is the fact that it contributes to the cutting edge of advances in technology. It belongs to the set of research that is developing the mathematical and technical infrastructure for future realization of greater capability. Current trends in technological advancement and deployment of autonomous machines (particularly in the military aerospace sector) clearly indicate a future of greater dependence on autonomous agents. As recently as the last decade the U.S. Air Force has progressed from deploying UAVs with a great deal of human intervention and control, to greater autonomy of UAVs and even arming UAVs such as the Predator with lethal weapons. An increasing number of munitions in Air Force inventories around the world are capable of autonomously performing tasks previously impossible without direct human intervention. Much like Billy Mitchell's visionary insight at the dawn of airpower in the United States, there is clear indication that in the near future, military powers will rely on unsupervised, autonomous platforms and munitions to carry out tasks, such as the search and destroy mission. This research is in direct support of this emergent capability.

In addition to the futuristic benefits of this research there are also immediate benefits to be gained from this thesis effort. A currently actionable outcome of this research is a set of analytical tools that may be used to assess the effectiveness of current operations in realistic, real-world search and destroy missions. The concepts developed in this work directly apply to current search and destroy operations, whether human or robotic. Specifically, the analytical tool developed by this research affords policy makers and war fighters a probabilistic assessment of desired target kill with consideration of the presence of false targets (either intentional decoys or otherwise misidentified targets). The theory and application to current assessment of concepts of operations (CONOPS) and rules of engagement (ROE) will be further developed and presented in section V of this thesis.

1.4 Background

In 1998, David Jacques and Robert Leblanc first formalized the stochastic theory enabling a more realistic assessment tool for the autonomous wide area search munition (WASM) in their paper, "Effectiveness Analysis for Wide Area Search Munitions" [5]. Traditionally, the effectiveness of a given munition was judged by the absolute probability of kill metric, P_k. The probability of kill was a subjective assessment that was bestowed upon a given munition. The main disadvantage of this metric (and motivation for Jacques and Leblanc's work) was that the P_k for a given munition did not consider the stochastic variation encountered by a munition in the real world. This discrepancy has become more notable and worthy of consideration with the increasing autonomy of munitions. In the authors' own words, "The single shot Pk numbers associated with most direct attack munitions are not directly applicable to wide area search munitions because they do not account for the difficulty of searching over tens of square kilometers in order to find a target of interest" [5]. The new theory incorporated the possibility of falsely classifying and attacking a target, or not detecting an intended target's presence at all. This probabilistic approach is necessary and useful when dealing with munitions capable of autonomously identifying and attacking targets, because the possibility exists that the automatic target recognition (ATR) and attack algorithms in the munitions may commit errors when subjected to the stochastic variation present in the real world.

Given the level of trust necessary to employ munitions in an autonomous search and destroy role at some point in the future, the success and hence the decision to use autonomous munitions will have to be judged by the probabilistic metric introduced above. It will be impossible to deterministically establish the effectiveness or success of a given munition. However, with readily available intelligence information about the munition's area of operation, probabilistic bounds on the success and failure (false target attack) of a given autonomous munition may be derived which would enable war fighters and policy makers to make decisions concerning the use of the munition. This analytical framework has been one of the main emphases of research in previous

years. In addition to this development, other work has been accomplished (using this probabilistic framework) to optimize the cooperative behavior of a swarm of munitions. Works by Gillen, Dunkel, Decker, and Kish [2–4, 7] have all been aimed at satisfying this objective. Specifically, their work, all accomplished at AFIT, has discovered mission efficiency gains by the optimization of various decision parameters such as when to cooperatively versus individually classify and attack based on scenario parameters. Further works by Jacques, Kish and Pachter [6, 9] have extended the idea of optimizing the mission efficiency of a swarm of autonomous munitions by addressing the optimal control of dynamically varying parameters. These parameters are variables that may be actively controlled or changed by the munition during the mission. Examples include, but are not limited to, sensor threshold, vehicle velocity, search pattern, sensor swath width, and ATR parameters. Work on optimal control of dynamically variable parameters has only begun very recently with the paper by Kish, Jacques and Pachter [9]. The main focus of my research will be to address some of the remaining gaps in this area of research.

1.5 Objectives

The objective of this research is to extend the results of the work on optimal control of munition sensor threshold that Kish produced in 2005 [7]. His original work showed that increasing mission efficiency was possible for a swarm of autonomous munitions by optimizing the sensor threshold. The impact of this research is discussed in greater detail in chapter II of this thesis. The objective of this research is to apply the results of the optimization to produce a WASM Operating Characteristic (WOC)—a performance metric for an autonomous WASM in a battlespace environment with false targets. Mission efficiency is gauged by the probability of attacking true, intended targets. At the same time it is important to avoid attacking false targets. In the case of a swarm of single-use munitions, a false target attack would result in a wasted munition - that is, a munition expended for no reason. This consequence is less severe in the case of multiple use munitions, such as a platform with multi-

ple warheads; however, the scope of this research is confined to single-use munitions. A false target could also contain adverse political value such as a hospital or civil structure. Attacking this type of false target is also undesirable, so the optimization of the probability of true target attack must be performed while at the same time constraining the probability of false target attack to an acceptable level.

As an example of this type of optimization, consider a munition sensitive to a particular type of target. The munition can vary its sensitivity to the unique characteristics of the target which uniquely identify it as that type of target. If the munition increases its threshold such that it is less sensitive to the target's characteristics, it will be more discriminating of false targets, because it will be more likely to dismiss false alarms of targets with similar attributes. However, the munition will coincidentally hamper its own ability to detect real targets. Thus the end result will be a decreased probability of attacking false targets, but also a decreased probability of attacking true targets. The converse may also be true if the threshold is lowered to allow consideration of more targets. In this case, the munition will increase its probability of identifying and attacking a true target, but it will at the same time increase the risk of being fooled by a false target. In addition to answering the optimal threshold balance question, the threshold optimization also affords other valuable insights. For instance, if a munition is close to the end of its time of flight and it has not encountered and detected any targets of interest, it is desirable (optimal, in fact) to lower the sensor threshold to allow consideration of a greater number of targets in the short time remaining for the target. Otherwise, if the munition keeps its threshold high, it will keep its probability of true target detection and attack low which increases the chances of wasting the munition. This scenario is commonly referred to as a go-for-broke tactic. Studying the results of the optimization and observing the implications yields these insights and more. A detailed treatment follows in the subsequent chapters.

1.6 Approach and Methodology

The approach to achieve the optimal control schedule for the dynamically variable sensor threshold of an autonomous munition in a search and destroy mission will use mathematical optimization techniques. Discrete optimization methods are used to corroborate the results of the continuous-time formulation. The theoretic framework established in the literature, which is based on the Poisson probability law, is well suited for closed form functional optimization and optimal control techniques. Special attention is paid to the closed form, continuous time methodology because it affords a great deal of insight in the performance and operating characteristic of an autonomous munition operating in the scenario in question. Gaining this insight is the objective of this thesis.

In reality, of course, any form of optimization may be used to achieve similar results. In previous work other methods such as the Response Surface Methodology have been successfully used to perform optimization [3, 4]; however, that optimization dealt with optimal decision rules, *not* optimal control. Standard optimal control techniques including Pontryagin's maximum principle and Lagrange multiplier techniques will be used for this problem since it enables closed form optimal solutions readily achievable considering the functional form of the autonomous search and destroy theoretical framework established in such works as [6]. In addition, this elegant optimization technique is immune to losses due to numerical imprecision and resistant to the opacity of meaning in the results that emerge from blindly exercising existing, commercial, computational optimal control algorithms.

1.6.1 Approach and Methodology: Assumptions. The various scenarios that describe a single munition or multiple autonomous munitions performing an autonomous search and destroy mission are established in [6] and elaborated in chapter II of this thesis. There are various scenarios, but for simplicity and to facilitate focus on the core problem of dynamically varying parameter optimization, only the

first scenario will be analyzed. This scenario is described by a single target uniformly distributed among a Poisson field of false targets.

1.7 Summary

The aim of this research is to establish optimal control algorithms for the dynamically varying sensor threshold of an autonomous munition performing a search and destroy mission. Perhaps one day the effectiveness of a swarm will be improved by applying methods so that optimally-acting individual agents may work cooperatively; however, the focus of this thesis remains on the individual agent. In addition, this research will support the development of theory which directly contributes analytical tools to gauge mission effectiveness of current assets, both manned and unmanned, performing similar missions in uncertain environments.

II. Supporting Background and Basic Principles

2.1 Overview

There is a great deal of research that has been accomplished in the field of cooperative control which encompasses several subtopics. Various companies, research agencies and universities have accomplished research that addresses the behavior of machines acting as autonomous agents in environments with varying degrees of real world representativeness. The literature available in support of the research contained in this thesis begins with Jacques and Leblanc's original work posing the stochastic performance evaluation analysis tool of autonomous munitions [5]. Further work, mainly carried out at AFIT, has built upon Jacques' theory and has introduced a sound, rigorous, theoretical framework for analyzing autonomous UAVs assigned to a search, classification and attack missions in a stochastic environment. Further work has addressed optimization of cooperative decision rule parameters as well as other characteristics of the environment and the autonomous agents operating within the environment. Additional optimization performed includes dynamically varying parameter optimization.

This chapter will discuss previous work that has been accomplished pertaining to the objectives of this research. Previous optimal decision rule determination as well as optimal control work will be highlighted. Most of this previous work has been accomplished at AFIT and this thesis serves as a follow-on to that foundation. In addition this chapter will also elaborate the theoretical and mathematical foundation of the optimal control problem ensuing in the following chapter. The chapter concludes with a proposition of the questions left remaining by the previous work and which gaps this research is aimed to address.

2.2 Scope

The topic of cooperative control implies a wide range of research options. The many subtopics of cooperative control for autonomous UAVs include formation flight (e.g. automated aerial refueling), path planning, task allocation, and cooperative

search, classification, and attack. The focus of this thesis is the optimal search and attack mission. Each of the subtopics is related in some way to each of the other topics and an overall cooperative control scheme must be able to efficiently execute each one; however, this research assumes that parallel behaviors and actions such as task allocation and path planning have been solved. What remains is the cooperative aspect dealing with optimal, collaborative search, classification, and attack. This scenario is called persistent area denial by Jacques and Pachter in [6]. Further scoping the problem, this research aims to establish optimal control schemes for individual UAVs so that the operating characteristic of the individual autonomous agent may be better understood and incorporated into a cooperative algorithm.

The following is an outline of the previous work that has been accomplished. This information is presented as a means of framing the current work in the context relative to the other research efforts that have taken place in the field of cooperative and optimal control.

2.2.1 Optimal Decision Rules. Using the same theoretical foundation presented later in section 2.3 as a foundation, work has been accomplished to establish optimal decision making policies for cooperative versus independent search, classification and attack. Consider circumstances such that a swarm of autonomous munitions or UAVs carrying munitions is released over a battle space. Each vehicle is capable of autonomously searching an area of the battle space. The vehicles possess the ability to detect targets with their array of sensors and subsequently submit the sensor data to an automatic target recognition (ATR) software package for target classification. This is how the vehicle determines if the detected object is a target or a false target. At that point the vehicle may choose to attack the target or request a cooperative classification attempt of the same target by a nearby vehicle. In uncertain environments, the cooperative classification may be beneficial, because multiple classifications of the target will produce a higher degree of confidence in the overall classification. The increased confidence will result in an increased probability of attacking true targets

and ignoring false ones. Likewise a certain vehicle may request a cooperative attack if it detects a target and deduces that it has a low probability of killing it with a single attack or if the vehicle determines that the target is a high priority.

The disadvantage of strictly cooperative behavior is that it requires greater resources, since the vehicle that was summoned (and agreed) to assist in cooperative activities forfeited its ability to continue searching and possibly detect additional targets. The threshold of cooperative activity may vary such that vehicles are more likely to accept cooperative behavior requests towards the end of the mission since the probability of encountering a target in the little remaining space to be searched is minimal. Likewise, in uncertain environments it may be considered more optimal to forfeit search opportunities in order to address cooperative classification attempts so that the probability of avoiding false target attack is increased. This may be especially important in politically sensitive environments. The variation and discovery of optimal combinations of all these parameters is the essence of the optimal decision rule work that has been carried out mainly at AFIT by Decker [2], Dunkel [3], Kish, Jacques, and Pachter [8], and Gillen [4].

2.2.1.1 Methodologies. Gillen's work specifically addressed the following objectives [4]:

1. Establish a methodology for measuring the expected effectiveness of a cooperative system of wide area search munitions.
2. Develop optimal cooperative engagement decision rules for a variety of realistic scenarios.
3. Analyze the sensitivities of the decision rule parameters to the precision of the munition's ATR algorithm, the lethality of the warhead, and the characteristics of the battlefield (clutter density, target layout, etc.).

Gillen's goal was to find the optimal combination of decision parameters. He used a computer simulation to assess the performance of the vehicles during the mission (i.e. mission success) as a function of the various decision parameters he was tuning. Gillen used an optimization technique called Response Surface Methodology

(RSM) to optimize the decision rules. RSM was particularly useful for this application because part of the process inherently enabled the accomplishment of the third objective cited above which was to analyze the decision parameter sensitivities to various scenario parameters [4].

Dunkel's work followed Gillen's and was closely related. Dunkel's research also used RSM, but made use of a different computer simulation to accomplish the following objectives [3]:

1. Develop a simulation that incorporates advantages as well as possible disadvantages of cooperative behavior.
2. Determine under what circumstances (munition and battlefield characteristic) it is beneficial to use cooperative behavior and under what circumstances it is detrimental to use cooperative behavior.
3. Determine the degree of benefit (if any) gained from cooperative behavior over non-cooperative behavior.

Both research efforts effectively showed an increase in mission efficiency by the use of decision rules optimized through the research. In addition, the latter work presented a sound analysis of the advantages, disadvantages, and general rules of thumb concerning the use of cooperative control strategies.

2.2.2 Dynamically Varying Parameter Optimization. Another area of optimization work that has been accomplished involves the optimal control for dynamically varying munition parameters. In particular, Kish's dissertation [7] solves the optimal control problem for determining the schedule of velocity and sensor threshold to maximize a munition's probability of attacking desired targets and avoiding attacking false targets. Most of the work leading up to Kish's dissertation assumes constant munition parameters. However, the design of autonomous wide area search munitions is conducive to varying certain operating parameters in order to achieve better performance as opposed to carrying out a mission with fixed, static settings of those parameters. For instance, consider the case of dynamically varying a munition's sensor threshold. The sensor threshold roughly corresponds to the sensitivity of the

sensor array to detect targets. Lowering the sensor threshold actually improves the chance of detecting targets but in doing so increases the likelihood of identifying noise (false targets) as true targets. Alternatively, increasing the sensor threshold decreases the probability of misidentifying false targets, but also decreases the overall ability to detect targets. The subject of this thesis follows on to Kish's work readdressing the optimal control solution methodology, paying special attention to continuous time formulation and solution methods, and interpreting the weapon operating characteristic results in a unique way.

The optimization problem is stated as follows [9]:

$$\begin{aligned} \max \quad & P_{TA} \\ \text{such that} \quad & P_{FTA} \leq P_{FTA_{max}} \end{aligned}$$

Qualitatively this means that it is desirable to increase the probability of attacking desired targets (P_{TA}) while absolutely constraining the probability of false target attack (P_{FTA}). This problem will be fully developed in the following chapters of this thesis. In [7], Kish develops and solves the problem for a variety of scenarios. The scenarios are described in section 2.3.1 of this chapter.

Kish's work affords several valuable insights. First, by considering various upper bounds on the probability of false target attack, one may observe the trend of the vehicle's tendency to commit to attacking an object that it has identified as a target. As one might expect, the higher the acceptable bound on $P_{FTA_{max}}$, the more likely the munition is to commit to an attack near the end of its time of flight. In other words, it lowers its sensor threshold toward the end of its mission to make it more probable that it will detect a target while at the same time increasing the risk (to the max acceptable level) of attacking a false target. In the endgame it might as well "go for broke" since, for a single-use munition at the end of its mission, if it has not committed to an attack it is wasted [9]. Comparing the results of the dynamic threshold optimization to the static threshold case shows clear improvements in mission efficiency by allowing a

dynamically variable sensor threshold. Likewise, Kish's work shows mission efficiency improvement by optimally varying other dynamic parameters, namely search area (velocity).

2.3 Foundation

Two key elements developed in the literature are central to this research. They are the Poisson probability distribution and the confusion matrix, which build up a framework for stochastic modeling of an autonomous UAV's environment. Much of the research in cooperative control to date has made deterministic assumptions. In most cases this has been necessary to demonstrate the main principles of that research without any additional, unnecessary complexity. The stochastic approach attempts to address an element of the realism associated with the actual, operational environment and develop optimal policies to execute in those scenarios. However, before these elements can be considered it is necessary to provide a context by establishing the *scenario*.

2.3.1 Scenarios. In order to meaningfully characterize a munition's performance it is necessary to model the environment in which it is operating. The battlespace (or operating environment) models are called scenarios. Each scenario describes a different set of mathematical assumptions including desired target distribution and false target distribution. In addition there are certain other characteristics that are assumed about the munition search. Those assumptions are discussed immediately following the list of scenarios. The scenarios and assumptions permit a tractable problem to be introduced and solved. Indeed, as is shown later in this thesis as well as in supporting literature, the mathematical assumptions are not unrepresentative of the real world. In addition, the assumptions and scenarios are designed to be calculated from readily available battlespace intelligence. For example, the Poisson probability distribution is a key element of the false target distribution model, see section 2.3.1.2, and the Poisson law parameter turns out to be the expected number

of false targets that the munition will encounter during its battlespace sweep. The Poisson probability law models a random number of encounters during a given time and is well suited to model a distribution of targets or false targets, because without further knowledge of the actual location of the false targets, the munition does not know when it will encounter the false targets. The Poisson distribution yields good results. Further evidence is presented in chapter V with verification in simulation and experimentation.

Some of the battlespace configurations that a munition may operate in are presented in [6] and are listed as follows:

- Scenario 1: A single target uniformly distributed among a Poisson field of false targets
- Scenario 2: A Poisson field of targets distributed among a Poisson field of false targets
- Scenario 3: A field of N targets uniformly distributed among a Poisson field of false targets
- Scenario 4: A field of N targets and M false targets, both classes uniformly distributed
- Scenario 5: A field of N targets normally distributed, centered on the origin, with some variance σ among a Poisson field of false targets
- Scenario 6: A field of N targets and M false targets, both classes normally distributed, centered on the origin, with target variance, σ_T, and false target variance, σ_{FT}

Kish's disseration [7] addresses several of these scenarios as well as additional complexities such as multiple warhead munitions. However, this thesis will concentrate on the detailed results of the weapon operating characteristic and to concentrate on this aspect only scenario 1 is considered for this research. The assumptions that accompany the scenario description for this thesis are that the munition has a single

warhead, or is a "single-use" munition, that the munition operates at a constant velocity, and that the battlespace search area is rectangular and the search pattern is exhaustive and non-duplicative. In other words, this thesis considers a munition with a dynamically variable sensor threshold in a battlespace environment with a single true target and a Poisson distribution of false targets. Scenario 1 is explained further in section 2.3.1.1.

2.3.1.1 Scenario 1. Scenario 1 is described as "a single target uniformly distributed amongst a Poisson field of False Targets (FT) in a battle space of area A_s" [6]. The parameters of interest are described in detail below. The results include a probability of a true target being attacked during the munition's sweep, the probability of mission success which is also dependent on a probability of kill derived from the specific munition's characteristics as well as the environment's state. Note that in this thesis the desired target of interest in the scenario 1 battlespace is often called the true target to more clearly distinguish it from false targets. The results also include the probability of a false target being attacked during the munition's sweep and the aggregate probability of anything being attacked during the mission (and conversely the probability that the munition survives the battle space sweep, which in the case of a single-use munition may very well indicate mission failure). By incorporating time intervals and integrating the aforementioned probabilities over the total mission duration additional information is presented such as the longevity of the munition in the case where it is expended, the probability of the munition lasting for a specified amount of time, the average longevity of a given target (or false target) in the battle space, and the average time for a target (or false target) attack to occur. These elementary probabilities are fully developed in [6].

Figure 2.1 illustrates the rectangular battlespace search area. The figure shows a munition (recall that in this thesis the munition only has one target attack opportunity, i.e. one warhead) with velocity v and sensor swath width w. The area A

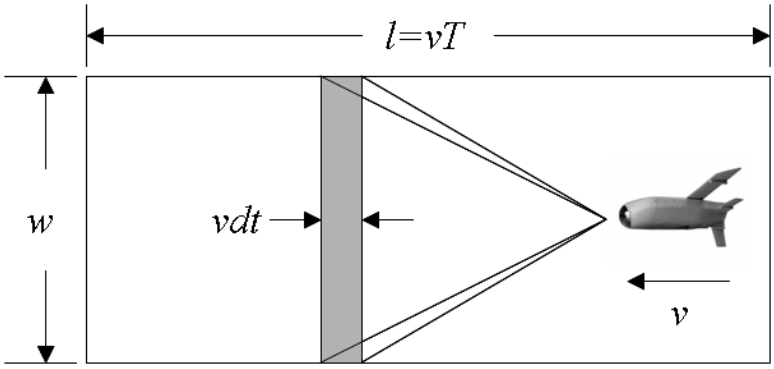

Figure 2.1: Exhaustive, non-duplicative, rectangular battlespace search area

searched up to time t is expressed as

$$A = wvt \tag{2.1}$$

and the total battlespace search area A_s for the searching occuring during $0 \leq t \leq T$ where T is the total battlespace search duration is

$$A_s = wvT \tag{2.2}$$

This paper's focus is on deriving a munition's optimal sensor threshold setting schedule to maximize the probability of attacking a true target during an engagement modeled by Scenario 1. First, consider the target encounter. The true target is uniformly distributed. This means that during an entire battlespace sweep the probability of encountering the true target at any given *location*, that is area increment, is given by $\frac{dA}{A_s}$. For instance, if units of kilometers are chosen to define the battlespace search area, A_s, and $A_s = 4\,km^2$ then the probability of encountering the target in any given square kilometer within the search area is $\frac{1}{4}$. Likewise, the temporal probability of true target encounter during a time interval of length dt is $\frac{dt}{T}$ where T is the time it takes to search the entire battlespace area. The false target distribution is modelled differently; the explanation follows.

2.3.1.2 Poisson Probability Distribution. The second outcome results from encountering a false target. The false targets are distributed according to a Poisson probability distribution. The Poisson random variable has a sample space, S, of all integers greater than or equal to 0, and the probability of exactly k encounters is given by the Poisson probability law

$$P(k) = e^{-\lambda}\frac{\lambda^k}{k!}, \quad k = 0, 1, 2, \ldots \quad \text{and} \quad \lambda > 0 \tag{2.3}$$

In terms of the false target distribution the Poisson probability law gives the probability of encountering k false targets within the search area. Obviously, an action that a munition may potentially take against a false target is conditioned upon first encountering that target. The Poisson probability law is commonly used in queuing theory and other rate-of-arrival type problems. This makes the Poisson probability law suitable for describing the false target encounters in the WASM scenario. The non-dimensional Poisson distribution's parameter, λ, is characterized in terms of density (number of false targets per unit area), $\alpha\left[\frac{1}{km^2}\right]$, such that when searching the area A

$$\lambda = \alpha A \tag{2.4}$$

The target density α can be readily discerned from current battlespace intelligence such as an Order of Battle. Let L equal the number of false targets assumed to be randomly distributed over a search area, A_s. Then,

$$\alpha = \frac{L}{A_s} \tag{2.5}$$

Furthermore, with the area searched up to time t from equation 2.1, the Poisson law parameter is readily derived from the available battlespace intelligence and munition operating characteristics

$$\lambda = \left(\frac{L}{A_s}\right) wvt \tag{2.6}$$

The Poisson probability law parameter is hence fully developed with basic information regarding the munition and the battlespace. Equation 2.3 may now be applied to yield a usable probability. For instance, to determine the probability of attacking the desired target (P_{TA}) it is necessary to know the probability that the munition did not previously attack a false target. The probability of false target attack (P_{FTA}) is the probability that the munition encounters a false target and incorrectly classifies it as the true target. Conversely, the probability that the munition does not attack any false targets, thus enabling it to attack the true target when it encounters it, is the probability of false target encounter (which is modeled with the Poisson probability law) times the probability that the munition correctly classifies the object as a false target. The probabilities of target and false target correct and incorrect classification conditioned upon encountering a given object are fully explained in section 2.3.2 with the topic of the confusion matrix. However, for now, suffice to say that the probability of correctly classifying a false target is P_{FTR}. Thus the probability of attacking exactly 0 false targets in the search area A is the probability that 0 false targets are encountered, plus the probability that exactly one false target is encountered and the munition correctly classifies it, plus the probability that exactly two false targets are encountered and correctly classified and so on for for any number of potential false targets up to ∞. This summation resulting in the probability of not attacking a false target ($P_{\overline{FTA}}$) may be expressed as

$$P_{\overline{FTA}}(A) = \sum_{k=0}^{\infty} P_{FTR}^{k} e^{-\lambda} \frac{\lambda^{k}}{k!} \tag{2.7}$$

Factoring and simplifying equation 2.7 and recognizing that

$$\sum_{k=0}^{\infty} \frac{(P_{FTR}\lambda)^{k}}{k!} = e^{P_{FTR}\lambda}$$

yields

$$P_{\overline{FTA}}(A) = e^{-\lambda(1-P_{FTR})} \tag{2.8}$$

The probability of not attacking any false targets $P_{\overline{FTA}}$ is a key piece of the mathematical foundation for the optimal control problem posed in chapter III. The probability $P_{\overline{FTA}}$ illustrates how the Poisson probability law is used to generate fundamental probabilities of interest.

2.3.2 Confusion Matrix and the Receiver Operating Characteristic. The second important element of the stochastic model buildup is the idea of the confusion matrix. The notion of identifying, or classifying, a false target was introduced in section 2.3.1.2 with the explanation of the Poisson probability distribution. The difference between real and false targets and the munition's correct identification of each upon encounter is really the crux of the stochastic model. Non-deterministic outcomes *must* be considered if one hopes to produce a realistic performance metric for an agent operating in a stochastic battlespace, i.e. the real world. To this end, a simple, binary confusion matrix is given below [6]:

Table 2.1: Binary confusion matrix: Probabilities of the munition classifying true and false targets conditioned on true or false target encounter.

	Encountered Object	
Declared Object	True Target	False Target
True Target	P_{TR}	$1 - P_{FTR}$
False Target	$1 - P_{TR}$	P_{FTR}

Table 2.1 shows the 4 probabilities associated with how a munition will classify (or declare) an object that it encounters in the battlespace. Complexity can be added to a confusion matrix by adding different types of targets. Adding such complexity adds one more row for each additional, specific type of target that the munition can encounter and a column for each different type of target for which the munition has a classification template. It is possible that there are more objects that is is possible to encounter than the munition knows to classify. The remainder of these "unknown" targets are grouped into a general false target class. Table 2.1 shows the most general example of a confusion matrix where consideration is paid solely to a single target

of interest and every other object that can possibly confuse the munition's sensor including purposefully deceptive false targets and environmental clutter is classified as a false target. The advantage of adding complexity is that it allows consideration of different types of target for, as an example, assessing the performance of a munition in attacking priority ranked targets. This thesis, however, will only consider the binary case.

Each of the values in the four cells of the confusion matrix is a conditional probability. The two fundamental probabilities are on the diagonal. P_{TR} is the probability that the munition correctly declares that it has detected a true (desired) target conditioned on the fact that it actually encounters a true target. Likewise, P_{FTR} is the probability that the munition correctly declares that it has detected a false (undesired) target, such as a decoy, conditioned on the fact that it actually encounters a false target. False targets include objects that are intentionally placed to deceive the munition as well as natural features inherent in the clutter of the battlespace that may cause the munition to incorrectly declare the presence of a true target. P_{TR} and P_{FTR} represent the two possibilities of correct target declaration that a munition may make based on its associated encounters. This is why the columns of the confusion matrix must sum to 1, because, for each type of target, true and false, there are only two possibilities of declaration. The off-diagonal elements are the error probabilities. The quantity $1 - P_{TR}$ is known as the false negative fraction, or the probability that the munition will commit a false negative error in the event that it encounters a true target. The quantity $1 - P_{FTR}$ is the false positive fraction, or the probability that the munition will commit a false positive error in the event that it encounters a false target. Mission success is defined by destroying real targets, thus, the confusion matrix plays a critical role in establishing the performance characteristics of a munition. The assumption is that anytime a munition declares a true target it will attack it, and anytime it declares a false target it will keep searching. Thus, the error probabilities are both detrimental because if the munition encounters a true target and declares it false, then it will miss the opportunity to attack the target resulting in mission failure.

Likewise, if the munition encounters a false target and declares it true, it will attack the false target, essentially wasting itself and eliminating any future probability of encountering the target of interest. In addition, this second error can also result in collateral damage if the attacked false target is a non-combatant.

As Jacques and Pachter [6] point out, the ideal confusion matrix would be no confusion at all, or, in other words, a perfect identity matrix. Ones on the diagonal and zeros elsewhere would indicate that all of the vehicle's sensor information was perfect, delivering the precise nature of the object that was detected. If the vehicle encountered a true target, it would *always* attack it leading to mission success whereas if it encountered a false target it would *always* declare it as such and choose to continue searching. Sadly, the perfect case is purely theoretical since an ideal confusion matrix is tantamount to omniscience. The ideal confusion matrix has no practical application because, unfortunately, the imprecision of sensors in general as well as the inaccuracy and ambiguity of automatic target recognition algorithms means that sometimes the vehicle will make an errant declaration. Errors will inevitably happen in actual scenarios which validates the reasoning behind the confusion matrix - especially the nontrivial case with non-zero off-diagonal elements.

In fact, the true nature of a munition's sensor is decidedly un-ideal. P_{TR} is like a threshold that the munition uses to discriminate objects that appear to be real targets and ones that don't. Note that in this example P_{TR} is inversely related to the sensor threshold level. That is, lowering the threshold level will cause the munition to consider more objects as real targets, i.e. it will be less discriminating, which will, in turn, increase the probability that the munition will make the correct declaration when it encounters a real target. However, P_{TR} is absolutely and inextricably related to the false positive fraction. Lowering the sensor's threshold, i.e. increasing P_{TR}, makes the munition less discriminant which unavoidably increases the munition's susceptibility to declaring a false target as a true target. In a real-world representation, P_{TR} is always monotonically increasing with $1 - P_{FTR}$ so increasing P_{TR} unavoidably pushes P_{FTR} further from its ideal value of 1.

The realistic sensor performance characteristic is described by a concept known as the Receiver Operating Characteristic (ROC). The ROC is the relationship between P_{TR} and the false positive fraction. The ROC that is used in this work is extracted from [9] and has been commonly accepted as a representative sensor characteristic for the subject munition systems. However, other ROC relationships may be used as long as they meet certain fundamental requirements. The ROC used here is given by

$$1 - P_{FTR} = \frac{P_{TR}}{c - (c-1)P_{TR}} \tag{2.9}$$

The ROC is parameterized by the non-dimensional scalar c which is a function of various operational and design characteristics. Basically, it describes how well the munition system is able to discriminate between true and false targets at a given sensor threshold setting. The higher the value of c, the better. Examples of aspects that affect c include munition velocity, sensor quality, ATR algorithm effectiveness, and target aspect, i.e. the amount of pixels that the sensor is able to detect based on the target's exposure. If the munition flies slower, it will most likely be able to capture more information on a given potential target by dwelling its sensor longer on the object which improves the sensor's chance of making a correct classification. Another example of improving the value c is installing a better quality sensor or ATR algorithm. It is more favorable to the munition if the sensor is able to better discriminate target features without adjusting its threshold. Figure 2.2 shows a family of ROC curves with varying values of c. Note that as c increases, the true to false positive ratio becomes more favorable.

Figure 2.2 also demonstrates the realism introduced to the problem by more accurately representing munition sensor characteristics, namely, avoiding the impossible ideal confusion matrix scenario. As previously mentioned, the concept of the ROC is heuristic so the ROC in equation 2.9 is not the only ROC that may be used, however, the given form has been shown to be empirically fit [11]. Also, the ROC used in this thesis meets the requirements for a valid ROC. First, the curve has to

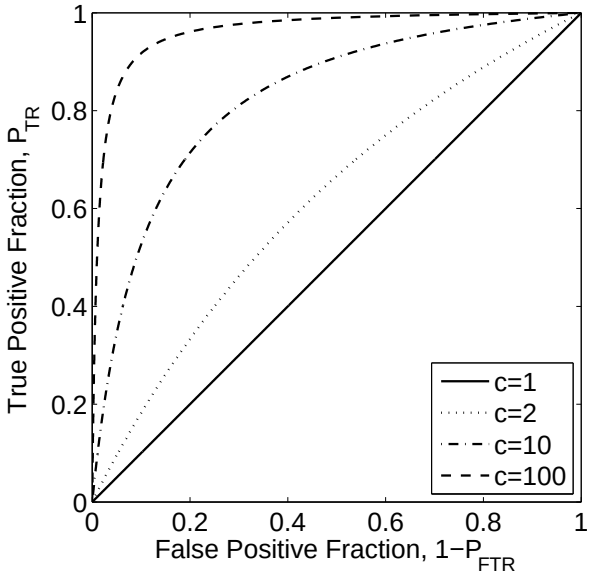

Figure 2.2: ROC curve for varying values of c

be monotonically increasing. In addition, the points $(0, 0)$ and $(1, 1)$ must exist (and bound) the curve. The meaning of the endpoints is important. Recall that the ideal theoretical confusion matrix is the identity matrix; however, ones on the diagonal of the confusion matrix would produce the ordered pair $(0, 1)$ on the ROC curve which only exists in the limit at $c \to \infty$. Essentially, the ROC says that in order to eliminate the possibility of committing a false positive error, the munition must also dismiss any probability of detecting a real target. On the opposite side, if the munition wants to make sure to detect the true target with probability 1, it must also accept that it has committed to attacking anything it sees.

A real-world munition may be flown in an artificial, test battlespace with representative true and false targets. The frequency of correct classifications at various sensor threshold settings may be used to populate various points which correspond to individual confusions matrices on a single ROC curve. A ROC curve can be empirically fit with equation 2.9 and the sensor quality parameter c can be solved. It is imperative that the sensor package be characterized well because the optimal sensor

threshold, which is the goal of this thesis, relies just as heavily on an accurate sensor characterization as the threshold itself.

The munition's sensor performance at a fixed threshold is characterized by a single confusion matrix. A ROC curve virtually represents an infinite number of confusion matrices. Adjusting the munition's sensor threshold varies P_{TR} and hence the munition's operating point on the ROC curve which is given by the ordered pair $(1-P_{FTR}, P_{TR})$. Dynamically varying the sensor threshold moves the operating point along the ROC curve which changes the munition's confusion matrix and the fundamental characterization of the munition and its sensor. The goal of the optimization in this thesis is to find the optimal schedule for varying P_{TR} such that, for a given c, the munition avoids attacking false targets and maximizes its probability of attacking the real one.

2.4 Summary

Over the past several years a sound theoretical foundation has been developed building on Jacques' and Leblanc's original research at Eglin AFB, FL. The resulting framework supports rigorous theory that provides analytical tools to assess the effectiveness of autonomous UAVs in a cooperative search, classification and attack function. In addition, multiple optimization efforts have been accomplished which present a cooperative decision rule optimization process as well as an analytical framework for the resulting optimal decision strategies. Also, optimal control work has identified ideal schedules for a munition's dynamically varying parameters. One of the key pieces of work in the optimal control area is Kish's dissertation [7]. This thesis will address a subset of the optimal control work presented in [7] by readdressing the Scenario 1 optimal dynamic sensor threshold problem paying special attention to the continuous time formulation and solution strategy as well as presenting the weapon operating characteristic in a unique and detailed way. Remaining questions include dynamic sensor threshold optimization combined with optimal decision policies for a

cooperative search, classification, and attack mission to be carried out by autonomous unmanned aerial vehicles.

III. Optimal Control of Dynamically Varying Sensor Threshold

3.1 Chapter Overview

Chapter II presented the core mathematical foundation from which the probabilities of interest, namely, P_{TA} and P_{FTA} as a function of a munition's dynamic controls, will be developed. Velocity can be varied, but in this thesis velocity is assumed constant and only sensor threshold is varied. Holding velocity constant is a simplifying assumption that allows one to focus on the weapon operating characteristic (WOC) results. This chapter builds on the foundation in chapter II by posing and solving the optimal control problem. The static optimization is presented first as a baseline where the optimal fixed sensor threshold is solved. The dynamic optimal control problem follows by first building the unconstrained problem and then adding a constraint on the maximum allowable probability of false target attack ($P_{FTA_{max}}$). This chapter concludes with the same, constrained optimal control problem posed as a discrete dynamic optimization problem. Solving the discrete formulation should corroborate the results of the continuous time solution. Chapter IV presents the results of the optimal control solution, namely the WOC and interprets the results. Chapter V concludes the thesis with a discussion of the results and and how the theory is applied to current operational scenarios.

3.2 Foundation

The objective of this thesis is to produce an optimal control *time* history maximizing the probability of true target attack in a given search space. Thus, from this point, temporal relationships will be adopted and probabilities relating to incremental areas will be abandoned. Indeed, they are interchangeable; however, in this work, probabilities relating to time will be used. In chapter II the Poisson parameter λ is developed as a function of the area searched, A, as in equation 2.4. Thus, with $\lambda \equiv \alpha A$, Equation 2.8 is presented in terms of incremental area. In order to transform

this to a probability dependent on time note that since $A_s = wvT$ and $A = wvt$,

$$A = A_s \frac{t}{T} \tag{3.1}$$

This makes sense as the area A searched by the munition up to time t is the search time fraction of the total battlespace search area (remember that a constant velocity munition is assumed). Furthermore, the overall desired search area for the probability in equation 2.8 is the munition's entire battlespace search area, A_s, thus let

$$\lambda = \alpha A_s \tag{3.2}$$

Combining equations 3.1 and 3.2 yields the desired parameter of the Poisson probability law

$$\alpha A = \lambda \frac{t}{T} \tag{3.3}$$

Then, from equation 2.8, the probability of not attacking any false targets as a function of time is given by

$$P_{\overline{FTA}}(t) = e^{-(1-P_{FTR})\lambda \frac{t}{T}} \tag{3.4}$$

The overall probability density function (pdf) corresponding to the probability, $f(t) \cdot dt$, that the intended target is attacked during the time interval, $[t, t+dt]$, is given by

$$f(t) = \frac{1}{T} P_{TR} e^{-(1-P_{FTR})\lambda \frac{t}{T}} \tag{3.5}$$

Another way of thinking of equation (3.5) is that the time of true target attack, t, is a random variable and $f(t)$ is its pdf. By component, the resulting probability from $f(t) \cdot dt$ is the probability that the true target has been encountered in that interval $(\frac{dt}{T})$ times the probability that the munition correctly classifies the encountered target (P_{TR}) times the probability that the munition has not previously engaged a false target $(P_{\overline{FTA}})$.

In the optimal control problem the probability of attacking the true target during the battlespace sweep will be the objective function to maximize. However, the achievement of this goal will be constrained by the probability of not attacking a false target. Thus the pdf, $g(t)$, for a false target attack must also be obtained. The probability, $g(t) \cdot dt$, of attacking a false target during the time interval $[t, t+dt]$ is the probability that the munition incorrectly classified the true target $(1 - P_{TR})$, also known as a false negative error, if it encountered it before time t, times the probability that the munition has not attacked a false target before time t $(P_{\overline{FTA}})$, times the probability that the munition encounters a false target during the time interval $[t, t+dt]$ and incorrectly classifies it (with probability $1 - P_{FTR}$), also known as a false positive error. Thus, the pdf

$$g(t) = \left[\left(1 - P_{TR}\frac{t}{T}\right)\right]\left[e^{-(1-P_{FTR})\lambda\frac{t}{T}}\right]\left[\frac{1}{T}\lambda(1 - P_{FTR})\right] \tag{3.6}$$

Several probabilities relevant to the WASM performance may be derived from the two fundamental probability density functions, $f(t)$ and $g(t)$, including the probability of mission success and the probability that the munition does not engage anything at all resulting in its survival of the battlespace sweep. These derivations are presented in Jacques and Pachter [6].

3.3 Static P_{TR}

The pdfs obtained in Section 3.2, lay the foundation for evaluating the probability P_{TA} of successfully attacking the intended true target. The objective is to maximize P_{TA} by optimally manipulating the sensor threshold-determined probability of target report P_{TR} while at the same time mitigating the consequence of increasing P_{TA}, which, unfortunately, is an undesirable simultaneous increase in the probability P_{FTA} of attacking a false target. For this investigation, which assumes a constant velocity munition, the munition's single control variable is the probability of target report, P_{TR}, which is equivalent to setting the munition's sensor threshold. The first

step in understanding the optimal control problem is to gain insight by addressing the static optimization problem, namely, the optimal setting of a constant P_{TR}.

As previously mentioned, the objective function to maximize is the probability of target attack during $0 \leq t \leq T$. The control variable is $P_{TR}(t)$, but for the static optimization a constant, optimal value, P_{TR}^{*}, is chosen for all t. Furthermore, since the control variable, P_{TR}, is a probability, it is constrained according to $0 \leq P_{TR} \leq 1$. Equation (3.5) is the pdf for the true target attack during a time interval of length dt beginning at time t, so to obtain the overall probability of target attack in the time interval of interest (the entire battlespace sweep) the pdf must be integrated. Thus, the performance function P_{TA} is given by

$$J \equiv P_{TA} = \int_0^T f(t)dt \tag{3.7}$$

For clarity, from here on the Poisson parameter λ, in equation (3.5), will be replaced with λ_{FT} to indicate that it is the Poisson parameter corresponding to the false targets' distribution in the battlespace. In addition, $f(t)$ should be in terms of the control variable, P_{TR}, so the term, $1 - P_{FTR}$, is eliminated using the sensor's ROC—equation (2.9). With these substitutions the static optimization problem is then

$$\max_{P_{TR}} \int_0^T \frac{1}{T} P_{TR} e^{-\left(\frac{P_{TR}}{c-(c-1)P_{TR}}\right)\lambda_{FT}\frac{t}{T}} dt \tag{3.8}$$

Non-dimensionalizing the time by setting $T := 1$ results in the payoff function

$$\max_{P_{TR}} P_{TR} \int_0^1 e^{-\left(\frac{P_{TR}}{c-(c-1)P_{TR}}\right)\lambda_{FT}t} dt \tag{3.9}$$

Integrating equation (3.9) yields the objective function

$$P_{TA}(P_{TR}) = \frac{1}{\lambda_{FT}} \left[c - (c-1)P_{TR}\right] \left[1 - e^{-\left(\frac{P_{TR}}{c-(c-1)P_{TR}}\right)\lambda_{FT}}\right] \tag{3.10}$$

Equation (3.10) is then the mission objective P_{TA} for given values of the problem parameters λ_{FT} and c. One seeks to select an optimal static control setting, P_{TR}, to apply throughout the mission.

In order to analyze constrained solutions, the expression for the probability of a false target attack, P_{FTA}, must also be derived. Following the same procedure for obtaining P_{TA}, the pdf of false target attacks, $g(t)$, must be integrated. Applying the same substitutions as before for λ and $1 - P_{FTR}$ into equation (3.6) and integrating yields the cost function

$$P_{FTA}(P_{TR}) = \int_0^T g(t)dt \tag{3.11}$$

$$= \left[1 - \frac{c-(c-1)P_{TR}}{\lambda_{FT}}\right]\left[1 - e^{-\left(\frac{P_{TR}}{c-(c-1)P_{TR}}\right)\lambda_{FT}}\right] + P_{TR}e^{-\left(\frac{P_{TR}}{c-(c-1)P_{TR}}\right)\lambda_{FT}} \tag{3.12}$$

The results, including the static WOC, are presented in chapter IV. Using equations 3.10 and 3.12, one can solve for the best possible probability of target attack during a munition's battlespace sweep given a maximum allowable probability of attacking a false target. This single munition performance metric is the essence of the WOC.

3.4 Dynamic P_{TR}

Section 3.3 presented and discussed the methodology and solution for obtaining the maximum probability of true target attack for a fixed sensor threshold, that is, a fixed P_{TR}. These results are useful; however, the design of wide area search munitions allows for dynamically varying the sensor's threshold. It is thus desirable to obtain the optimal dynamic P_{TR} schedule such that the mission probability of target attack is maximized. This optimal control problem is analyzed in Sections 3.4.1 and 3.4.2. First, the continuous time formulation and solution will be presented. The elegance and simplicity of the Poisson probability distribution permits a continuous time,

closed-form optimal control solution to be obtained. The continuous solution will be corroborated in the following section by a discrete time formulation and numerical solution using MATLAB®.

3.4.1 Continuous Optimal Control Problem. Similar to the static case in Section 3.3, the unconstrained problem will be analyzed first followed by the inclusion of the constraint on the probability of false target attack.

3.4.1.1 Unconstrained Case. The unconstrained optimal control problem statement is

$$\max_{P_{TR}} P_{TA}$$

Recall from before that the objective, P_{TA}, is the integral of the pdf of true target attack during the battlespace sweep. Recalling equation (3.7)

$$\begin{aligned} P_{TA} &= \int_0^T f(t)dt \\ &= \int_0^1 ue^{-\int_0^t \lambda_{FT}\frac{u}{c-(c-1)u}d\tau}dt \end{aligned} \tag{3.13}$$

Note that in the problem formulation the following notation is used

$$u \triangleq P_{TR}$$

Also, as before, the objective function is normalized by setting $T = 1$. Finally, note that the exponent has been replaced with the equivalent integral form to facilitate the state definition. By introducing the state dynamics as

$$\dot{x} = \frac{u}{c-(c-1)u},\ x(0) = 0,\ 0 \le t \le 1 \tag{3.14}$$

and recognizing that

$$x = \int_0^t \dot{x}dt = \int_0^t \frac{u}{c-(c-1)u}dt \tag{3.15}$$

the problem statement can be rewritten as

$$\begin{aligned} \max_{u} \quad & P_{TA} = \int_0^1 u e^{-\lambda_{FT} x} dt \\ \text{subject to} \quad & \text{the dynamics (3.14)} \end{aligned} \tag{3.16}$$

The Hamiltonian is formed by appending the dynamic constraint to the objective with a costate, λ_x,

$$H = u e^{-\lambda_{FT} x} + \lambda_x \frac{u}{c - (c-1)u} \tag{3.17}$$

The costate differential equation is

$$\dot{\lambda_x} = -\frac{\partial H}{\partial x} = \lambda_{FT} u e^{-\lambda_{FT} x}, \ \lambda_x(1) = 0 \tag{3.18}$$

From equation (3.18) it can be seen that the costate is monotonically increasing since its time derivative is always positive. Combining this fact with the costate boundary condition, also given in Equation (3.18), one infers that

$$\lambda_x(t) < 0, \ 0 \leq t < 1 \tag{3.19}$$

The same type of insight can be derived from the state dynamics. It can be shown from equation (3.14) that the state, x, is monotonically increasing since its derivative is always positive. Since the initial value of the state is $x(0) = 0$, $x(t) > 0$ for all $0 < t \leq T$. These insights will be useful in characterizing the solution. The optimality condition is

$$\frac{\partial H}{\partial u} = 0 = e^{-\lambda_{FT} x} + \lambda_x \frac{c}{[c - (c-1)u]^2} \tag{3.20}$$

The optimal control is obtained by solving for u in equation 3.20 and is given by

$$u^* = \frac{-\left(\sqrt{-\lambda_x c}\right) e^{\frac{1}{2}\lambda_{FT} x} + c}{c - 1} \tag{3.21}$$

One may confirm that this extremum yields the desired maximum of the Hamiltonian by observing

$$\frac{\partial^2 H}{\partial u^2} < 0,\ 0 \leq u \leq 1 \tag{3.22}$$

Substituting the optimal control, u^*, from equation (3.21), into the state and costate dynamics from equations (3.14) and (3.18), gives the two point boundary value problem

$$\dot{x} = -\frac{1}{c-1}\left(1 - \frac{\sqrt{c}}{\sqrt{-\lambda_x}e^{\frac{1}{2}\lambda_{FT}x}}\right),\quad x(0) = 0,\ 0 \leq t \leq 1 \tag{3.23}$$

$$\dot{\lambda_x} = \lambda_{FT}\sqrt{-\lambda_x}ce^{-\frac{1}{2}\lambda_{FT}x}\dot{x},\qquad \lambda_x(1) = 0,\ 0 \leq t \leq 1 \tag{3.24}$$

The idea is to solve the two point boundary value problem posed by equations (3.23) and (3.24) which would return the optimal state and costate trajectories which could then be used to plug into the equation for the optimal control in equation (3.21) to produce the optimal control schedule. The solution method is presented below where the two equations are reduced to a single differential equation that is a function of the state variable x and an initial guess of the final state value. This final form of the TPBVP can easily be solved using a single shooting method especially since the state dynamics are transparent and provide ample insight as to which direction to adjust the initial guess and converge on a solution. However, there is a problem that is insidiously present in equations (3.23) and (3.24) which does not become apparent until consideration of the fact that the optimal control schedule is not continuous in its first derivative, i.e. it is piece-wise smooth but has a corner. Specifically, the optimal control is subject to the laws of probability and is bounded in the interval $[0, 1]$. This results in an inevitable time that the control will saturate in the unconstrained problem. The principle behind the control saturation including the saturation time and its impact on the problem will be investigated later in this section. For now, suffice to say that the TPBVP in the form of equations (3.23) and (3.24) ignores the existence of a time where the optimal control schedule does not obey equation (3.21).

The solution method following from equations (3.23) and (3.24) is presented below as it is mathematically correct and illustrates a solution methodology pitfall that is easy to overlook; however, the solution is only actually valid when the control saturation time is identically equal to 1 which only occurs when $c = 1$ which is outside the set of valid values for c. The recommended solution methodology is presented at the end of this section.

What follows is the *faulty* solution methodology that ignores the existence or possibility of a control saturation. In theory it is a promising solution methodology because the dynamics of the state are fairly well understood; therefore, the TPBV problem can be solved using the single shooting method with insights from the state dynamics driving the initial guess for convergence of the shooting method. First the system of differential equations is reduced to a single differential equation that is a function of a single variable and unknown boundary conditions. In this case, the costate differential equation can be solved in terms of x and $x(1)$ and substituted back into the state differential equation to apply the shooting method. Letting

$$y \triangleq -\lambda_x$$

the following expression is formed from equation 3.24

$$\frac{\dot{y}}{\sqrt{y}} = -\lambda_{FT}\dot{x}\sqrt{c}e^{-\frac{1}{2}\lambda_{FT}x} \tag{3.25}$$

Recognize that

$$\frac{d}{dt}\sqrt{y} = \frac{1}{2}\frac{\dot{y}}{\sqrt{y}}$$

and that

$$\sqrt{c}\frac{d}{dt}e^{-\frac{1}{2}\lambda_{FT}x} = -\frac{1}{2}\sqrt{c}\lambda_{FT}\dot{x}e^{-\frac{1}{2}\lambda_{FT}x}$$

It can now be shown that

$$\frac{d}{dt}\sqrt{y} = \sqrt{c}\frac{d}{dt}e^{-\frac{1}{2}\lambda_{FT}x} \tag{3.26}$$

Integrating both sides yields

$$\sqrt{y} + Const = \sqrt{c}\left[e^{-\frac{1}{2}\lambda_{FT}x} + Const\right] \tag{3.27}$$

which reduces to

$$y = c\left(e^{-\frac{1}{2}\lambda_{FT}x} + Const\right)^2 \tag{3.28}$$

Substituting the previous definition for y in equation 3.28 results in

$$-\lambda_x = c\left(e^{-\frac{1}{2}\lambda_{FT}x} + Const\right)^2 \tag{3.29}$$

The final step is to apply the costate boundary condition, $\lambda_x(1) = 0$, which results in the costate solution in terms of the state variable, x, and its unknown boundary condition, $x(1)$,

$$\lambda_x = -c\left[e^{-\frac{1}{2}\lambda_{FT}x} - e^{-\frac{1}{2}\lambda_{FT}x(1)}\right]^2 \tag{3.30}$$

Though the process is mathematically correct thus far, the inconsistency with the requirements for a valid control schedule, namely $0 \leq P_{TR} \leq 1$, first appear in equation (3.30). Even though the costate requirement for a free-final-state optimal control problem, that $\lambda_x(1) = 0$, was enforced in producing equation (3.30), the underlying assumption that is present is that the resulting solution variable, $x(1)$, is the final value of the state trajectory solution for equation (3.23), which has incorporated one and only one form for the optimal control which is given in equation (3.21). The substitutions that have led up to and supported equation (3.30) do not permit any modifications or modal changes outside of what is permitted by equation (3.21). Thus the solution is automatically invalidated if $u^* = 1$ for any time $t < 1$ which is demonstrated below to *always* occur for the unconstrained solution. The inconsistency is not readily apparent if one solves the problem using this solution methodology for parameter combinations of c and λ_{FT} that produce a saturation time close to 1. High expected numbers of false targets, which directly corresponds to high values of λ_{FT}, yield solutions that saturate late. The reason that the inconsistency is not readily

apparent in these cases is because the invalid solution methodology is correct for the theoretical case where the saturation time is identically equal to 1 and the disparity grows as the difference $1 - t_c$ grows, where t_c is the saturation time. In cases where the solution is found for parameter combinations of c and λ_{FT} that produce an early saturation time the disparity is obvious: the resulting optimal control schedule is clearly outside the bounds of a valid probability.

With careful consideration of the insight presented above, substituting the solution for λ_x from equation (3.30) back into the state differential equation (3.23), we see that the optimal state trajectory is given by

$$\dot{x} = \frac{1}{c-1} \cdot \frac{1}{e^{\frac{1}{2}\lambda_{FT}[x(1)-x]} - 1}, \; x(0) = 0, \; 0 \leq t \leq 1 \tag{3.31}$$

The form of the optimal state trajectory from equation (3.31) can be used with the single shooting method to make an initial guess of $x(1)$, propagate the dynamic equation, adjust the guess and finally converge on the optimal state trajectory by eventually matching the $x(1)$ guess to the final, propagated state value. However, before doing this, consider that as $t \to 1$, $x(1) - x \to 0$. Therefore, it can be seen from equation 3.31 that

$$\lim_{t \to 1} \dot{x} = \infty$$

This curious result may imply an irregularity at the final time. Recalling the boundary condition for the costate, $\lambda_x(1) = 0$, it can be seen from equation 3.21 that

$$u^*(1) = \frac{c}{c-1} > 1$$

when P_{FTA} is not bounded, i.e. in the unconstrained case. Furthermore, analyzing the time derivative of the optimal control reveals that $\dot{u^*} > 0$ which means the optimal control is monotonically increasing. This is a usual trait of optimal control problems, but in this case the control, $u = P_{TR}$, is a probability, so at the critical time t_c it saturates at 1, its maximum value, and maintains that value until the final time.

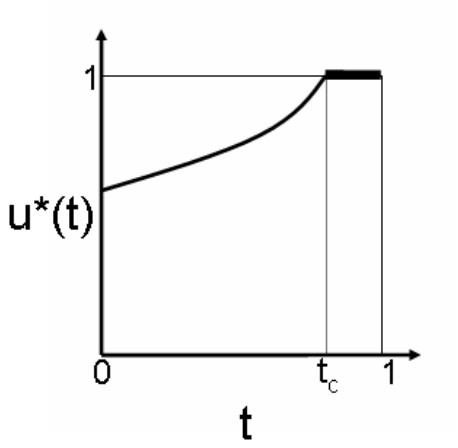

Figure 3.1: General trend of optimal control and annotation of critical saturation time

The critical time is what is referred to as the "saturation time" above. In related literature [9] this endgame behavior of the optimal solution is termed "going for broke." Intuitively, it makes sense: if the munition has not yet correctly identified the true target, and so far it has managed to avoid attacking any false targets and thus destroying itself, the munition will lower its sensor threshold (increase P_{TR}) to try to identify anything at all in the final moments of the engagement. After all, an unused munition is a wasted munition. The saturation time t_c depends on the expected density of false targets in the battlespace (set by the value of λ_{FT}). This concept will be further developed later.

The general behavior of the optimal control described in the previous paragraph is illustrated in Figure 3.1. In order to use the shooting method to calculate the optimal control and/or state trajectory, it is necessary to find the critical time, t_c, when the optimal control saturates, that is, P_{TR} assumes the value 1. The optimal state trajectory will then be propagated in two parts, the first part for the time interval $0 \leq t < t_c$ according to the state trajectory determined by equation (3.14) with $u = u^*$, and the second part for the time interval $t_c \leq t \leq 1$ also determined by equation (3.14) but with $u^* = 1$.

By definition

$$u^*(t_c) = 1 \tag{3.32}$$

Substituting this value into the equation for the state dynamics, equation (3.14), gives

$$\dot{x}(t) = 1,\ t_c \leq t \leq 1 \tag{3.33}$$

Integrating equation (3.33) and applying the final condition yields the following endgame optimal state trajectory (where endgame denotes the period during the battlespace sweep when the munition's sensor threshold is low as well as saturated, i.e. $P^*_{TR} = 1$)

$$x(t) = t + x(1) - 1,\ t_c \leq t \leq 1 \tag{3.34}$$

The solution for t_c is found from the solution to equation (3.34) at time t_c as well as by solving for the costate solution at the same time, $\lambda_x(t_c)$. The optimal endgame state trajectory, equation (3.34), is substituted into the costate differential equation, equation (3.18), along with $u^*(t_c) = 1$ resulting in

$$\dot{\lambda_x} = \lambda_{FT} e^{-\lambda_{FT}(x(1)-1)} e^{-\lambda_{FT} t},\ \lambda_x(1) = 0,\ t_c \leq t \leq 1 \tag{3.35}$$

Integrating equation 3.35 and applying its boundary condition gives

$$\lambda_x(t) = e^{-\lambda_{FT} x(1)} \left(1 - e^{\lambda_{FT}(1-t)}\right) \tag{3.36}$$

Making the appropriate substitutions for $x(t_c)$ from equation 3.34, $\lambda_x(t_c)$ from equation 3.36, and $u^*(t_c) = 1$ into the formula for the optimal control from equation 3.21 and solving for t_c yields

$$t_c = 1 - \frac{1}{\lambda_{FT}} \ln\left(\frac{c}{c-1}\right) \tag{3.37}$$

It is important to note several insights from the solution for t_c. First, t_c is obviously bounded in the search interval between 0 and T, which in this normalized

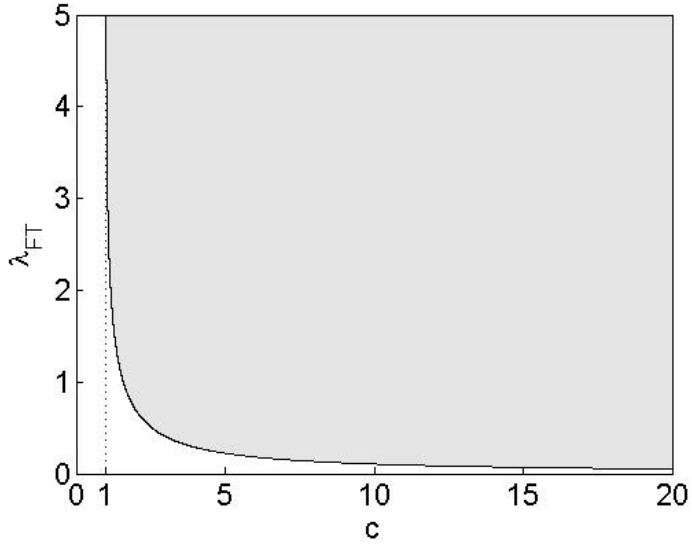

Figure 3.2: Feasible parameter domain for c and λ_{FT}

case is $0 < t_c < 1$. The upper bound, $t_c < 1$, can be reduced to yield $c < \infty$. This makes sense by considering the ROC (equation 2.9). A value of $c = \infty$ would mean that the acquisition sensor was absolutely perfect meaning that it was capable of never making a false-positive error while at the same time being able to discriminate true targets. This contradicts the ROC concept as, from before, the true target declaration (P_{TR}) and the false-positive fraction ($1-P_{FTR}$) are equal at the points $(0, 0)$ and $(1, 1)$.

The lower bound of t_c is more useful. The bound $t_c > 0$ reduces to the following direct correspondence between c and λ_{FT}

$$\lambda_{FT} > \ln\left(\frac{c}{c-1}\right) \tag{3.38}$$

This curve is plotted in Figure 3.2. The relationship between c and λ_{FT} indicates that one may not arbitrarily choose corresponding values. As λ_{FT} decreases (indicating that the munition expects to see a sparser density of false targets) to very small values, the munition must have reasonably good sensor characteristics to expect to see anything at all. Likewise, if the munition is equipped with an extremely poor sensor (low value for c), it makes little sense to release this munition in search of a target

interspersed among a low density of false targets because there is a high probability that the munition will be wasted, unable to find the target by the time the battlespace search is over. Indeed, it is an even worse decision to release a munition with a poor sensor to search an area with a high density of false targets as it will be difficult to mitigate the probability of attacking one while maintaining a reasonable probability of attacking the desired true target. This undesirable outcome is namely because as the quality of the sensor c decreases, t_c also decreases indicating a sooner go for broke time which is the last action the munition should consider in a battlespace with poor sensor characteristics. The other important insight regarding the parameters' impact on the optimal control saturation time t_c is that lowering the false target density λ_{FT} will advance the saturation time while increasing the expected false target density will delay it. In other words, if the munition expects a lower density of false targets it can afford to go for broke sooner without an undue risk of encountering any false targets during the remainder of the mission. In summary, t_c varies proportionately with c and λ_{FT}.

As previously noted, the solution method outlined in equation (3.23) through equation (3.31) is erroneous. The best solution method is to solve the two point boundary value problem summarized below. The two differential equations are comprised of the original form of the state and costate differential equations. The optimal control is given in equation (3.21). If using the shooting method there are two possibilities: shooting forward and backward. If shooting forward, make an initial guess for the costate. Propagate the state and costate incrementally calculating the optimal control at each time step which is used to calculate the next increment of the state and costate. At the final time compare the value of the costate to the known boundary condition, $\lambda_x(1) = 0$. With the previously gained insights on the state and costate dynamics, lower the initial costate guess if the final costate results in a positive value. Alternatively, one may solve the same problem with a reverse shooting method. To implement the reverse shooting method apply the costate boundary

condition, $\lambda_x(1) = 0$, and propagate the state and costate backwards until time $t = 0$. Iterate until the initial condition on the state, $x(0) = 0$, is met.

The shooting method propagation must be accomplished in two parts, from time $0 \leq t < t_c$, and the remainder, $t_c \leq t \leq 1$. Alternatively, the state and costate may be propagated until the optimal control, a function of the state and costate value at each increment saturates, then $u^* = 1$ until the final time. Using this method, t_c is not predetermined, but the mode changes based solely on enforcing the constraint $u^*_{max} = 1$ on the control. Solving the problem with or without t_c predetermined results in the same solution.

The following is a summary of all the final equations for the unconstrained, continuous-time, optimal control history for $P^*_{TR}(t)$.

$$\dot{x} = \begin{cases} \frac{u}{c-(c-1)u}, & x(0) = 0,\ 0 \leq t < t_c \\ 1, & x(t_c) = x(t_c),\ t_c \leq t \leq 1 \end{cases} \tag{3.39}$$

$$\dot{\lambda_x} = \begin{cases} \lambda_{FT} u e^{-\lambda_{FT} x}, & \lambda_x(0) = \lambda_x(0),\ 0 \leq t < t_c \\ \lambda_{FT} e^{-\lambda_{FT} x}, & \lambda_x(1) = 0,\ t_c \leq t \leq 1 \end{cases} \tag{3.40}$$

$$u^*(x, \lambda_x) = \begin{cases} \frac{-\left(\sqrt{-\lambda_x c}\right) e^{\frac{1}{2}\lambda_{FT} x} + c}{c-1}, & 0 \leq t < t_c \\ 1, & t_c \leq t \leq 1 \end{cases} \tag{3.41}$$

3.4.1.2 Constrained Case. Having obtained the unconstrained solution, it naturally follows to seek the constrained solution which will deliver the optimal control schedule to maximize the same objective as before while at the same time mitigating (i.e. constraining) the probability of attacking a false target. With this in mind, the problem statement changes to the following

$$\begin{aligned} \max_u \quad & P_{TA} \\ \text{such that} \quad & P_{FTA} \leq P_{FTA_{max}} \end{aligned}$$

Recall the pdf $g(t)$ from equation (3.6)

$$g(t) = \frac{1}{T} \cdot \frac{\lambda_{FT} u}{c-(c-1)u} \left(1 - \frac{1}{T}\int_0^t u d\tau\right) e^{-\frac{1}{T}\lambda_{FT}\int_0^t \frac{u}{c-(c-1)u} d\tau} \tag{3.42}$$

Note that in equation (3.42) the following substitutions have been made—the control u is defined as

$$u \triangleq P_{TR},$$

the term, $1 - P_{FTR}$, has been replaced with the ROC curve relationship from equation (2.9), and the time-dependent terms have been expressed in their integral forms. As before, the integral form requires the introduction of the state dynamics

$$\dot{x} = \frac{u}{c-(c-1)u}, x(0) = 0, 0 \leq t \leq 1 \tag{3.43}$$

$$\dot{y} = u, \qquad y(0) = 0, 0 \leq t \leq 1 \tag{3.44}$$

Recalling equation (3.11) and substituting the state definition in for the integral terms in $g(t)$ (see equation 3.15) yields the constraint

$$P_{FTA} = \int_0^1 \frac{u\lambda_{FT}}{c-(c-1)u}(1-y)e^{-\lambda_{FT}x} dt \tag{3.45}$$

where the battlespace sweep time T has been non-dimensionalized setting it equal to 1. The objective function for the constrained problem is modified by adding the equality constraint imposed by the probability of false target attack, P_{FTA}, with a Lagrange multiplier, λ

$$\max_u J = \int_0^1 u e^{-\lambda_{FT}x} + \lambda \frac{u\lambda_{FT}(1-y)}{c-(c-1)u} e^{-\lambda_{FT}x} dt \tag{3.46}$$

Note that in this formulation the constraint is appended as an *equality* constraint. This means that the solution, $u^*(t)$, will only be optimal insofar as it is not more beneficial in terms of the probability of target attack to use the unconstrained solution rather than the constrained solution forcing the probability of false target attack to

the value specified as the required $P_{FTA_{max}}$. The resulting P_{TA} for a mission is not unique in P_{FTA} except at the optimum meaning that a munition can achieve the same P_{TA} but with two distinctly different outcomes for the penalty, P_{FTA}. Clearly, the solution that results in a lower P_{FTA} is desirable. Choosing the problem formulation with P_{FTA} as an equality constraint as in equation (3.46) will result in a solution that *forces* the resulting P_{FTA} to the specified value. As has been previously shown with the ROC, there is an advantage in raising the allowable P_{FTA} to a certain point since raising the value of the constraint permits a better outcome for the objective functional as well. However, at some point it is no longer optimal and the best solution that can be obtained is the unconstrained solution. This approach, setting the constraint as an equality, is also related to the penalty approach. The final constraint will be set by tuning the value of the Lagrange multiplier, λ, $\lambda < 0$, until the resulting value for P_{FTA} matches the maximum allowed for the mission. If the maximum is greater than value of P_{FTA} produced by the optimal unconstrained solution, then the latter will be used and the constraint will be inactive. Note that the penalty approach method, namely, posing the $P_{FTA_{max}}$ constraint as an equality constraint was chosen in lieu of posing the same constraint as an inequality. The complexity in adding a slack variable by posing the constraint as an inequality was probably preserved in the form of additional work to ensure that for a given parameter combination the optimality of the solution was maintained. The conditions to ensure optimality are presented later in this section.

The Hamiltonian for the constrained case is formed by appending the two constraints imposed by the dynamics equations, with their associated costates, to the modified objective function given in equation (3.46)

$$H = ue^{-\lambda_{FT}x} + \lambda\frac{u\lambda_{FT}(1-y)}{c-(c-1)u}e^{-\lambda_{FT}x} + \lambda_x\frac{u}{c-(c-1)u} + \lambda_y u \tag{3.47}$$

Applying Pontryagin's Maximum Principle, the optimal control is found by solving for u^* in the following

$$\frac{\partial H}{\partial u} = 0 = e^{-\lambda_{FT}x} + \lambda \frac{\lambda_{FT}(1-y)c}{[c-(c-1)u]^2} e^{-\lambda_{FT}x} + \lambda_x \frac{c}{[c-(c-1)u]^2} + \lambda_y \tag{3.48}$$

Likewise, the costate differential equations are found by taking the derivative of the Hamiltonian with respect to the states

$$\dot{\lambda_x} = -\frac{\partial H}{\partial x} = \lambda_{FT} u e^{-\lambda_{FT}x} \left[1 + \lambda \frac{\lambda_{FT}(1-y)}{c-(c-1)u}\right], \lambda_x(1) = 0 \tag{3.49}$$

$$\dot{\lambda_y} = -\frac{\partial H}{\partial y} = \lambda \frac{u\lambda_{FT}}{c-(c-1)u} e^{-\lambda_{FT}x}, \qquad \lambda_y(1) = 0 \tag{3.50}$$

In the interest of verifying the optimality of the solution, the second partial derivative of the Hamiltonian with respect to the control is given by

$$\frac{\partial^2 H}{\partial u^2} = 2c(c-1)[c-(c-1)u]^{-3} \left[\lambda(1-y)\lambda_{FT} e^{-\lambda_{FT}x} + \lambda_x\right] \tag{3.51}$$

To ensure that the optimal solution is indeed a maximum the sufficient condition is checked

$$\frac{\partial^2 H}{\partial u^2} < 0 \; \forall \; u^* \tag{3.52}$$

The sufficient condition is determined by examining the various terms in equation (3.51). The necessary condition for the constraint to be met according to the method of Lagrange multipliers, is that $\lambda < 0$. In addition, it can be determined from the initial condition $y(0) = 0$ and the bounds on the control, and hence $\dot{y}$, $0 \leq \dot{y} = u \leq 1$ that $0 < y < 1$. The remaining variable is λ_x, which, by removing the (always positive) leading term in Equation (3.51) and rearranging, can be seen to meet the sufficient condition in Equation (3.52) when

$$\lambda_x < -\lambda(1-y)\lambda_{FT} e^{-\lambda_{FT}x} \tag{3.53}$$

Unlike the unconstrained solution presented in section 3.4.1.1 where it was shown that this condition was always met, the constrained solution may or may not be optimal depending on the value of the states and costates. The real insight is obtained by looking at Equation (3.53) again in a slightly rearranged form

$$\lambda < -\frac{\lambda_x}{\lambda_{FT}(1-y)e^{-\lambda_{FT}x}} \tag{3.54}$$

In tuning the value of the Lagrange multiplier to achieve the desired $P_{FTA_{max}}$ reducing (making more negative) the value for λ tightens the constraint forcing $P_{FTA_{max}}$ to a lower allowable value. Increasing λ, i.e. making it less negative, increases (relaxes) the constraint allowing a higher $P_{FTA_{max}}$. In essence, tuning the value for λ varies the penalty imposed by P_{FTA} in the modified cost function (equation 3.46). As previously discussed, since $P_{FTA_{max}}$ is set up as an equality constraint in this problem, increasing $P_{FTA_{max}}$ beyond a certain point invalidates the optimality of the solution as the corresponding mission P_{TA} peaks and then begins to decrease with increasing P_{FTA}. At this point the second partial in equation (3.51) switches sign invalidating the condition in Equation (3.52). Equation (3.54) provides a bound on λ identifying the valid range of values to ensure an optimal solution while meeting the P_{FTA} constraint. When acquiring a solution, λ may be tuned to any value to adjust the desired $P_{FTA_{max}}$ constraint as long as the value for λ meets the condition in Equation (3.54).

From equation (3.48) the optimal control is

$$u^* = \frac{\sqrt{c}}{c-1}\left[\sqrt{c} - \sqrt{-\frac{\lambda(1-y)\lambda_{FT} + \lambda_x e^{\lambda_{FT}x}}{1+\lambda_y e^{\lambda_{FT}x}}}\right] \tag{3.55}$$

The optimal control, u^*, is a function of 4 variables: x, y, λ_x, and λ_y. The problem is shaping up to be a complex TPBV problem. The problem can be simplified somewhat by reducing the dependence on at least one of the variables, λ_y. This reduction is only possible for the constrained case for combinations of parameters (i.e. c, λ_{FT}, $P_{FTA_{max}}$) that do not force the control to saturate ($u^* = 1$) before the end of the mission. For the

cases where the saturation does occur, which more closely resemble the unconstrained solution, the set of differential equations representing the states and costates must be integrated in a bimodal fashion. The reason is due to the existence of the time t_c which is always present in the unconstrained solution. Reducing the variables assumes a single set of differential equations valid for time $0 \leq t \leq T$. Reducing the variable dimension in the following way ignores the existence of t_c which is why this solution step must not be used for the unconstrained solution, or for parameter combinations in the constrained solution such that the control saturates before the end of the mission. The method for finding the critical time, t_c, will be addressed later.

For valid parameter combinations seeking the constrained solution the following method to reduce the dimension of the problem makes the resulting TPBV problem more tractable in the event that solving the TPBV problem is the solution method of choice, or alternate methods are unavailable. The target variable to reduce is λ_y. Observe that the state differential equation for x, equation (3.43), can be substituted into the costate differential equation for λ_y, equation (3.50). The resulting equation is

$$\dot{\lambda_y} = \lambda_{FT}\lambda\dot{x}e^{-\lambda_{FT}x} \tag{3.56}$$

Recognizing that

$$\frac{d}{dt}\left(-\lambda e^{-\lambda_{FT}x}\right) = \lambda_{FT}\lambda\dot{x}e^{-\lambda_{FT}x} \tag{3.57}$$

and integrating both sides yields

$$\lambda_y = -\lambda e^{-\lambda_{FT}x} + Const,\ \lambda_y(1) = 0 \tag{3.58}$$

After applying the boundary condition and solving for the integration constant the resulting solution is in terms of x and $x(1)$—a single state trajectory

$$\lambda_y = \lambda\left[e^{-\lambda_{FT}x(1)} - e^{-\lambda_{FT}x}\right] \tag{3.59}$$

The solution for λ_y in equation (3.59) can be substituted into the previous equations for $\dot{x}$, $\dot{\lambda_x}$, and $\dot{y} = u^*$, equations (3.43), (3.49), and (3.55) respectively. With these substitutions the dimension of the TPBV problem is reduced, but the complexity in terms of satisfying the boundary conditions imposed by the equations has been preserved. Eliminating the dependence on λ_y transferred the requirement to converge to $\lambda(1) = 0$ to $x(1) = x(1)$ where the final value in the x state trajectory must be equal to the initial guess for $x(1)$ which is one of the independent variables resulting in equation (3.59).

One can find the solution of the TPBV problem in x, y, and λ_x by first choosing a value for λ. This value directly corresponds to the $P_{FTA_{max}}$ constraint. This value can be adjusted later by tuning λ. Remember that as the solution of the state and costate differential equations are propagated it is important to continually check the validity of the value for λ by making sure that it meets the condition specified in equation (3.54). The initial conditions for x and y are given in equations (3.43) and (3.44), respectively. Choose an initial guess for $\lambda_x(0)$ and $x(1)$ and propagate, or integrate, the differential equations, also called "shooting". Converging on the final solution that satisfies the boundary conditions (and for which optimality is guaranteed), requires iterating the above steps until the conditions have been met. As with the unconstrained solution the nature of the state and costate equations affords some insight as to how to adjust the initial guess to come closer to the solution with each iteration. Given that the x state differential equation is always positive, x is monotonically increasing from $x(0) = 0$. The correct initial guess for $x(1)$ lies somewhere between the guess and the actual, final propagated value of the x state trajectory. The variable y is positive and monotonically increasing with the initial condition, $y(0) = 0$, and, as previously noted, the sign of the λ_x costate trajectory varies depending on the optimality of the solution. Care must be taken to pursue the solution with insight into the convergence of the solution and the solution itself. For instance it would be wise to solve the unconstrained problem first. If the P_{FTA} that results from an attempt to obtain the constrained solution is higher than that resulting from the unconstrained case it

means that either the process is not converged, one should choose a different value for λ—the $P_{FTA_{max}}$ constraint, or the unconstrained solution yields the best performance that can be achieved with the selected values for c and λ_{FT}.

As previously noted, the method outlined above to obtain the constrained solution should only be used when there does not exist a time $t_c < 1$ when $u^*(t_c) = 1$. This is the case for *most* constrained solutions; however, the time t_c is found as follows. Recalling the equation for the optimal control, $u^*(t)$ (3.55), and noting that $\lambda_x(1) = 0$ and $\lambda_y(1) = 0$

$$u^*(1) = \frac{\sqrt{c}}{c-1}\left[\sqrt{c} - \sqrt{-\lambda[1-y(1)]\lambda_{FT}}\right] \tag{3.60}$$

The question is, for what value of λ is $u^*(1) > 1$. This question is posed mathematically as

$$1 < \frac{\sqrt{c}}{c-1}\left[\sqrt{c} - \sqrt{-\lambda[1-y(1)]\lambda_{FT}}\right] \tag{3.61}$$

The set of valid values for λ is less than or equal to zero, so solving for λ, $u^*(1) > 1$ when

$$-\frac{1}{c\lambda_{FT}[1-y(1)]} < \lambda \leq 0 \tag{3.62}$$

If the condition in equation (3.62) is met there exists some time t_c less than 1. As with the unconstrained solution method, the state and costate solutions may be propagated with our without the predetermination of t_c. If it is determined that t_c exists, the solution may be propagated until the control equals 1, which marks the critical time, t_c. For the remainder of the integration $u* = 1$. The mode changes based solely on enforcing the constraint for a valid control, $0 \leq u^* \leq 1$. Otherwise the time t_c may be predetermined in which case the solution is propagated with $u = u^*$ from $0 \leq t < t_c$ and $u^* = 1$ from $t_c \leq t \leq 1$. Both solution methods yield identical results.

If t_c exists, it is found in a way similar to the unconstrained case presented in Section 3.4.1.1. First, knowing that $u^*(t_c) = 1$ and substituting it into the equations

for the state dynamics, equations 3.43 and 3.44, yields the endgame state trajectories

$$x(t) = t + x(1) - 1,\ t_c \leq t \leq 1 \tag{3.63}$$

$$y(t) = t + y(1) - 1,\ t_c \leq t \leq 1 \tag{3.64}$$

Substituting the state solutions given in equations 3.63 and 3.64 into the costate differential equations given in 3.49 and 3.50 and integrating yields solutions for the costate trajectories in the time interval $t_c \leq t \leq 1$. Substitute the solutions for $x(t_c)$, $y(t_c)$, $\lambda_x(t_c)$, and $\lambda_y(t_c)$ into the expression for $u^*(t_c)$ from equation 3.55 and solve for t_c resulting in

$$t_c = 1 - \frac{1}{\lambda_{FT}} \ln \left[\frac{\lambda}{c(1+\lambda)} + \frac{\lambda_{FT}}{1+\lambda} \left[1 + \lambda\lambda_{FT}(1 - y(1)) + \lambda \right] \right] \tag{3.65}$$

One observation to note is that the resulting solution for t_c and the condition for the existence of t_c (equation 3.62) are both dependent on $y(1)$ which is the integral of the control. Intuitively, this indicates that as the constraint $P_{FTA_{max}}$ is relaxed the area under the sensor threshold schedule curve increases. For a given parameter combination (i.e. c and λ_{FT}) there is some point at which the area captured by the optimal control schedule curve grows to a point where the control will go for broke before the end of the mission. As the area under the curve grows even more the go for broke time t_c occurs earlier.

3.4.2 Discrete Optimal Control Problem. The two-point boundary value problem proves very challenging, especially as the complexity and dimensionality of the optimal control problem increases. For this reason an alternate solution method will be demonstrated that entails a discretized version of the problem and a subsequent solution by means of a numerical optimization algorithm.

The Mayer formulation of the discrete-time optimal control problem [1] is given by

$$\min_{u(i),i=0..N-1} \phi[\underline{s}(N)] = -P_{TA}$$

$$\text{subject to}$$

$$\underline{s}(i+1) = f[\underline{s}(i), u(i), i]$$

$$\psi[\underline{s}(N)] = P_{FTA} \leq P_{FTA_{max}}$$

where $\underline{s}$ represents the state vector $\begin{bmatrix} x \\ y \end{bmatrix}$. In the Mayer form the path cost (a sum of incremental probabilities) is represented as a single terminal cost. From Equation (3.16) the discretized objective, P_{TA}, becomes

$$\phi[x(N)] = \Delta t \sum_{i=1}^{N} u(i-1) e^{-\lambda_{FT} x(i-1)} \tag{3.66}$$

In the same way, from Equation (3.45) the discrete problem constraint, P_{FTA}, is

$$\psi[\underline{s}(N)] = \Delta t \sum_{i=1}^{N} \frac{\lambda_{FT} u(i-1)}{c-(c-1)u(i-1)} [1-y(i-1)] e^{-\lambda_{FT} x(i-1)} \tag{3.67}$$

The discretized state equations are given by

$$x(i+1) = x(i) + \Delta t \frac{u(i)}{c-(c-1)u(i)} \tag{3.68}$$

$$y(i+1) = y(i) + \Delta t \; u(i) \tag{3.69}$$

Discrete optimal control problems are solved by representing the continuous time formulation in terms of a cost at each discrete time step of interest, or an overall path cost sum, that is is a function of a number of states at each time step as well as a control vector at each time step. The control vector becomes the parameter vector to vary in the resulting static, parameter optimization problem. The optimization may be solved

by a number of algorithms, but for the purposes of this investigation MATLAB's 'fmincon' gradient-search algorithm proved robust and fast enough to accurately and efficiently find the optimum control vector that agreed with the analytic solution.

3.5 Summary

Chapter III presents and solves the problem to determine the optimal P_{TR} setting maximizing the probability of attacking the true target and avoiding the false target attack outcome. Chapter IV presents the results of the optimization, namely, the Weapon Operating Characteristic (WOC) and its interpretation and meaning with regards to a munition's performance in a battlespace with the presence of false targets.

IV. The Wide-Area Search Munition Operating Characteristic

4.1 Overview

Chapter III presented the optimal control problem and its solution for an optimal fixed and dynamic P_{TR}. The objective is to characterize a munition so as to obtain its best possible probability for attacking the true target in Scenario 1 given a constraint on the probability of the undesirable outcome of attacking a false target. This chapter presents the wide-area search munition operating characteristic (WOC). First the static WOC resulting from the solution in section 3.3 is presented followed by the dynamic WOC from the solutions presented in section 3.4 and a comparison of the static and dynamic results.

4.2 Static Results

Recall equation 3.10, the mission objective P_{TA} for given values of λ_{FT} and c. The optimum, without concern for the ensuing P_{FTA}, which will eventually become the constraint, may be found by solving for the value of P_{TR} that equates the derivative with respect to the control, P_{TR}, of equation (3.10) to zero. Alternatively, one can observe the peak of the curve plotted in Figure 4.1. Figure (4.1) shows a peak at $P^*_{TA} = 0.535$, which, for $\lambda_{FT} = 25$ and $c = 100$ maximizes the probability of target attack. This unconstrained optimum is achieved by applying the fixed, unconstrained optimum sensor threshold corresponding to $P^*_{TR} = 0.723$ for the duration of the munition's search and attack mission. The peak and subsequent decline in P_{TA} make sense because increasing the control past the optimum (analogous to lowering the sensor threshold beyond the optimum level) substantially inhibits the munition's probability of reaching the true target (which it would probably classify correctly since P_{TR} is set so high) before encountering a false target and incorrectly classifying it (recall that the false positive fraction, $1 - P_{FTR}$, increases with P_{TR} according to the ROC relationship) resulting in an attack on the false target.

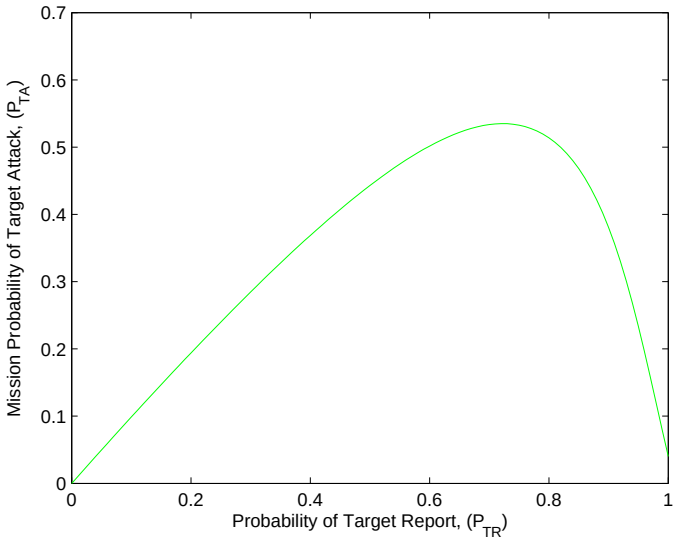

Figure 4.1: Mission P_{TA} vs static P_{TR}; $\lambda_{FT} = 25$, $c = 100$

Adding the constraint derived in equation 3.12, Figure (4.2) overlays the probability of false target attack obtained from plotting equation (3.12) as a function of P_{TR}. In addition, the probability of not attacking anything at all (i.e. the munition survives the battlespace sweep) as a function of P_{TR} is also plotted. This curve, derived from the resulting probability given by the expression $1 - P_{TA} - P_{FTA}$, is monotonically decreasing, as expected, just as the probability of false target attack is monotonically increasing.

Figure 4.2 shows the cost that is incurred in terms of the probability of attacking undesired false targets in the battlespace while attempting to find and attack the true target. Thus, the maximum P_{TA} can be determined for a given mission constrained by a maximum allowable probability of false target attack, P_{FTA}. For instance, it can now be seen that the overall, unconstrained, optimal probability of target attack for the mission (from Figure 4.1), $P^*_{TA} = 0.535$, incurs a cost of $P^*_{FTA} = 0.318$. However, suppose that the maximum allowable P_{FTA} is bounded at 0.2; the optimal constrained solution is now a static $P^*_{TR} = 0.563$ with a resulting $P^*_{TA} = 0.483$.

With the static optimization complete it is now possible to obtain the overall WASM Operating Characteristic (WOC). The WOC shows the optimum achievable

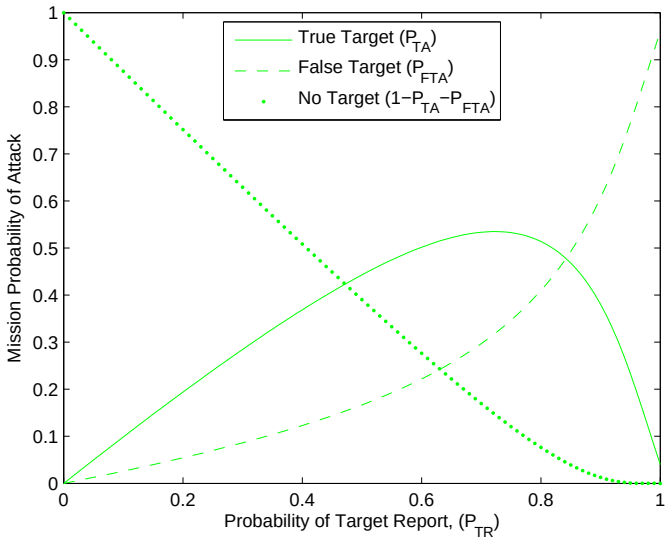

Figure 4.2: Mission probability of attack with constant P_{TR} for $\lambda_{FT} = 25$, $c = 100$. Plots show probability of attacking a true target, a false target, and no target at all.

P_{TA} for a given bound on P_{FTA}. This is analogous to the classical ROC from the theory of communication. The WOC, however, is specific to the munition of interest as it quantifies its overall mission effectiveness with respect to parameters of interest, namely P_{TA} and P_{FTA}. The WOC for a munition's optimal, but fixed, sensor threshold setting is shown in Figure 4.3. This will also be the goal of the dynamic optimization in Section 3.4 in addition to the optimal sensor threshold control schedule to achieve the best objective/cost tradeoff.

The WOC in Figure 4.3 corroborates and readily shows that which can be inferred from Figures 4.1 and 4.2. First, the WOC is not a monotonically increasing function. The optimum, unconstrained P_{TA} is clearly seen at the peak of the curve which matches the optimum value cited earlier as well as the corresponding value of P_{FTA}. In addition, the WOC clearly shows at which point the value of the constraint, P_{FTA}, should be capped. This also occurs at the peak of the curve since mandating any further increase in the probability of false target attack only hinders the achievement of the objective, namely maximizing the probability of true target attack (note that this only applies if the problem is solved posing the $P_{FTA_{max}}$ constraint as an equality

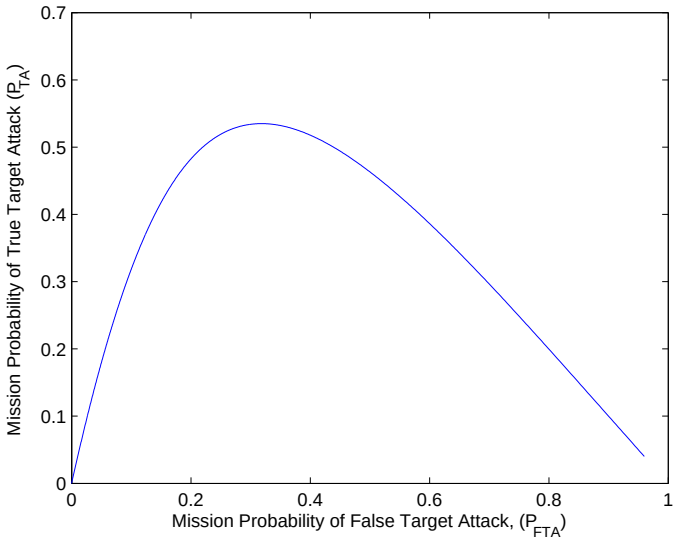

Figure 4.3: Static WASM Operating Characteristic (WOC); $\lambda_{FT} = 25$, $c = 100$

as in this thesis). Indeed the same probability of true target attack may be achieved by two separate selections of P_{TR}; however, the lower solution is clearly better since the higher value results in a higher probability of false target attack. In practical terms this means that as the sensor threshold is reduced (P_{TR} is increased) there is some point at which the unconstrained solution should be used since it delivers the highest probability of target attack.

4.3 Dynamic Results

This section continues with the results garnered from solving the optimal control problem solved in Section 3.4. The dynamic WOC sheds a substantial amount of insight into the performance of wide-area search munitions operating in a battlespace environment containing false targets.

The key result is the WASM Operating Characteristic, or WOC, which gives information similar to the classical ROC specific to the performance of an autonomous search and attack munition. Comparing the results presented in Figure 4.3 to the optimal, dynamically varying sensor threshold setting shows the improvement gained by applying the optimal control approach. Figure 4.4 compares the baseline case where

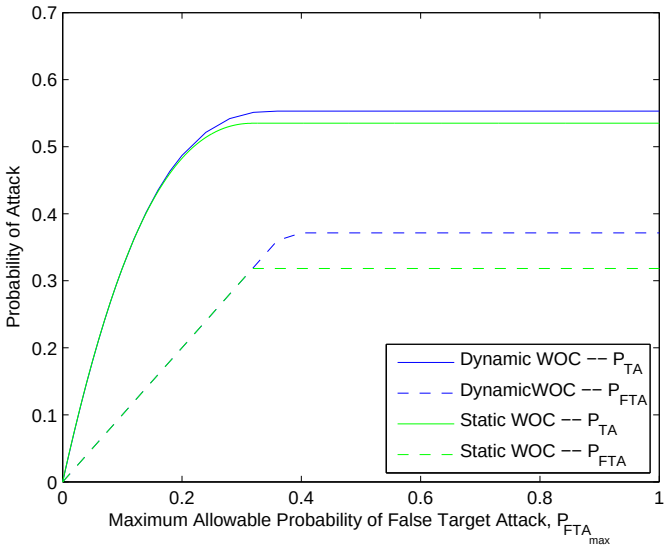

Figure 4.4: Static and Dynamic WOC, $\lambda_{FT} = 25$, $c = 100$.

the problem parameters are $c = 100$ and $\lambda_{FT} = 25$. This is the same parameter combination as in Figure 4.3. There are several things to note from this example. First, note the obvious improvement in P_{TA} in the dynamic case which applies the optimal schedule for the varying sensor threshold. Various parameter combinations show different levels of improvement, but several things stand out. Optimally varying the sensor threshold always produces a higher probability of target attack than maintaining the sensor threshold at an optimal, albeit constant level throughout the mission. The improvement is very noticeable as $P_{FTA_{max}}$ is increased; however, even at lower values of the max allowable false target attack probability, the P_{TA} resulting from optimally varying the sensor threshold is improved, but it is too small to notice in the figure. The reason for this is that as the constraint is lowered, i.e. a lower $P_{FTA_{max}}$ is imposed, the dynamic optimal control solution (P_{TR} schedule) shifts downward as well as flattens looking more and more like the static solution. Indeed, one can infer from the ROC that the trivial case represented at the origin of the ROC, where the maximum allowable probability of false target attack is zero, would have identical dynamic and static solutions: flat lines of $P_{TR} = 0$ from $0 \leq t \leq T$. The other trait present in all static vs. dynamic WOC comparisons is that with an increase in the ob-

jective P_{TA}, there is also an increase in P_{FTA} when the solution is not constrained by $P_{FTA_{max}}$. Presumably this would be acceptable since the chosen $P_{FTA_{max}}$ is actually the maximum allowable probability. This concept also relates back to ROC insights. The ROC indicates that the objective and the penalty unavoidably vary together in a way governed by c, the parameter that is set by the quality of the sensor, ATR algorithm, munition velocity, pixels on target, etc. Practically, the static solution is only constrained up to a certain point where it is no longer beneficial to allow a higher probability of attacking a false target during the mission since the munition is already doing the most it can to that end. At that maximum, the unconstrained solution is used. The same is true for the dynamic solution, however, it can take advantage of a higher P_{FTA} constraint since the dynamic solution can achieve a higher P_{TA} than the static one. In cases where the $P_{FTA_{max}}$ constraint is set low enough that both the static and dynamic solutions are constrained, the resulting P_{FTA} for both solution cases is equal, but the dynamic solution still yields a higher P_{TA}.

Another point to note in Figure 4.4 is that the WOC curves flatten at a certain point corresponding to the transition to the unconstrained, optimal P_{TR} schedule. Fortunately it is intuitive, but it is important to remember because in the following figures the WOC will be presented only as the P_{TA}, $P_{FTA_{max}}$ relationship. The P_{FTA}, $P_{FTA_{max}}$ relationship is always one of equality until the breakpoint where P_{FTA} remains constant for the remaining values of $P_{FTA_{max}}$. Thus for any desired value of $P_{FTA_{max}}$ the resulting P_{FTA} may also be inferred by just looking at the single P_{TA}, $P_{FTA_{max}}$ WOC.

The following figures are surface plots illustrating several WOCs. Each individual WOC is a slice of the surface in the $P_{FTA_{max}}$-P_{TA} plane. The WOCs, and therefore the surface, vary with the sensor's parameter c. Each surface varies with the number of assumed false targets, which is specified by λ_{FT}.

The first thing to note from Figures 4.5, 4.6, and 4.7 is the WOC trend as c varies. Holding λ_{FT} constant, the surface rises with c. This means that the WOC

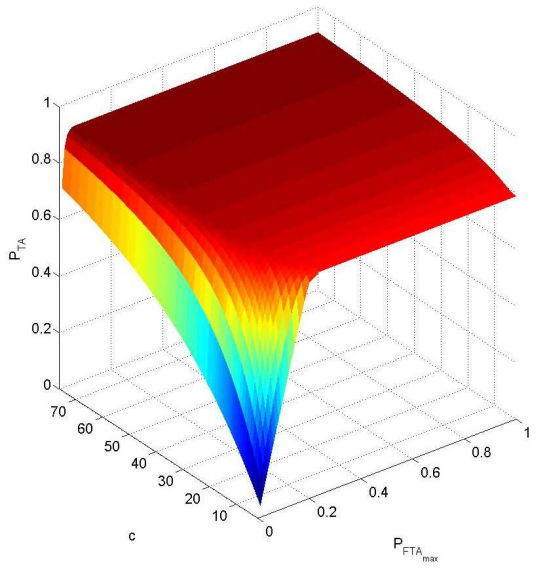

Figure 4.5: Dynamic WOC surface, $\lambda_{FT} = 0.5$.

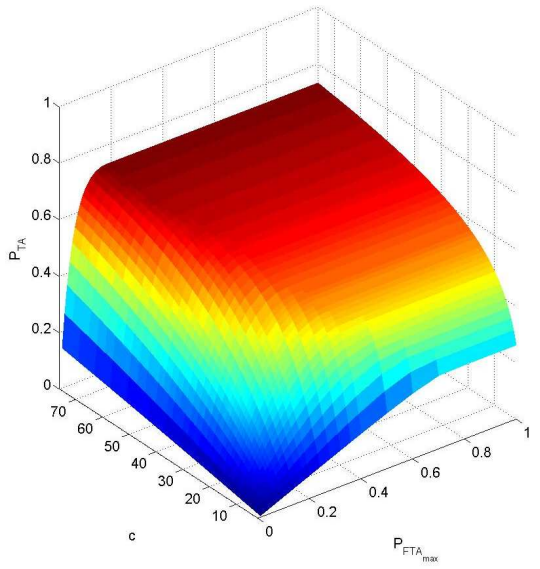

Figure 4.6: Dynamic WOC surface, $\lambda_{FT} = 5$.

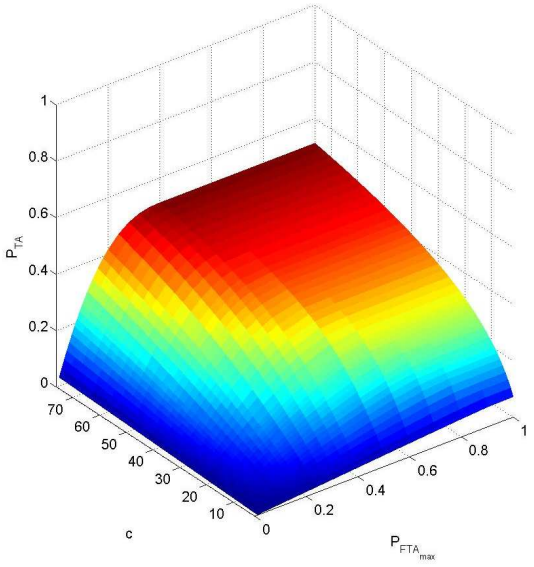

Figure 4.7: Dynamic WOC surface, $\lambda_{FT} = 25$.

becomes more favorable with higher values of c. The munition can achieve higher probabilities of true target attack without sacrificing as much in terms of the probability of attacking a false target. This makes sense because higher values of c mean that the munition's sensor is more capable of distinguishing true targets from the chaff without committing false positives. The result is that the munition implements higher P_{TR} schedules, or goes for broke earlier, without an undue risk of making a false positive error on an unintended (false) target. Higher values of c are realized by making it easier on the munition's sensor, that is, flying lower or slower and effecting more pixels (or observation time) on each potential target, improving the automatic target recognition algorithm, or improving the quality of the sensor itself. Another point to note is that with increasing c the WOC curve gets steeper. This translates directly to the effect on the ROC curve with increasing values of c. The munition performs better without being subject to higher values of $P_{FTA_{max}}$. Another way to think of this is that with higher c the munition achieves its unconstrained best at lower values of $P_{FTA_{max}}$. Otherwise, with poor sensor characteristics, the only way

for the munition to improve its objective (P_{TA}) is to eat up more P_{FTA}—the essence of the ROC (and hence WOC) relationship.

The other important insight garnered from the WOC surfaces is the trend that occurs with changes in the battlespace environment, namely, λ_{FT}. As λ_{FT}, or the expected number of false targets in the battlespace, increases the plotted surface lowers. Also, the steepness of the WOC decreases, i.e., the value of $P_{FTA_{max}}$ that the munition achieves its unconstrained best increases. In the interest of making sound operational decisions, one can observe this shift and obtain a feel for the $\frac{c}{\lambda_{FT}}$ ratio. One might decide that this ratio should be no less than 4, for example, indicating that the munitions ability to classify true targets has to be at least as good as a certain level dictated by the ratio relative to the expected number of false targets in the battlespace. This is a direct way that this theoretical research affects the policy of conducting autonomous search and attack operations.

The downward shift in the WOC surface with increasing λ_{FT} indicates that if the value chosen for λ_{FT} is an *over-estimate* of the actual number of false targets in the battlespace the probability of false target attack will always be less than the specified $P_{FTA_{max}}$. It will no longer be optimal, but it will most likely be close to optimal, and more importantly there is insurance that the maximum allowable probability of attacking an unintended object will be upheld. In other words, in the presence of uncertainty as to the density of actual false targets the munition will encounter in the battlespace, it is wiser to overestimate the expected number in order to preserve $P_{FTA_{max}}$. Mathematically, this is expressed as

$$P_{FTA} \leq P_{FTA_{max}} \quad \forall \quad \lambda_{FT} \leq \lambda_{FT_{max}} \tag{4.1}$$

4.4 Summary

The WOC *is* the performance characteristic for a properly characterized munition (quantified by the value for c) assigned to attack a target in a battlespace containing false targets. The WOC surfaces include the sensor quality information

as well allowing the potential for observing the characteristic for a range of c if there is some uncertainty in the weapon characterization. The following chapter discusses the application of these results as well as simultaneous efforts in simulation and experimentation that build on the theory presented in this thesis.

V. Conclusions

5.1 Overview

Applying optimal control techniques to the autonomous munition scenario is not only fascinating but practically applicable as well. Two concurrent theses written at AFIT have taken this theoretical research one step closer to practical application with a verification of the theoretical results in this thesis using a high-fidelity simulation as well as experimental validation. This chapter discusses the practical application of this theoretical work as well as the work that was completed simultaneously. The chapter concludes with recommendations for future work.

5.2 Application of Theory

Chapter I proposed a futuristic scenario where autonomous munitions are trusted to perform battlespace search and attack operations. In that scenario the munition may calculate it's optimal parameter variations in real time or the optimal schedule may be predetermined. In any case, the munition would perform an optimal battlespace sweep. The futuristic scenario is the direct application of the optimal sensor threshold schedule solution. However, there is a practical application of this theory that can be realized now. The scenario models are realistic mathematical representations of battlespace search and attack operating areas. Also, the Poisson distribution conveniently provides an accurate mathematical model for encountering randomly distributed false targets. Despite intelligence efforts, battlespace environments remain highly uncertain and, at times, unpredictable. Thus, the probabilistic approach and stochastic element introduced by the confusion matrix and ROC concept is often the best representation of a search and attack battlespace.

In light of the fact that this theory is a fairly good representation of the real world, the optimal solutions derived in this thesis provide a baseline for current operations. Commanders and others who depend on munitions or other vehicles, both manned and unmanned, to perform search and/or attack type missions have a probabilistic expectation for the performance of their systems operating in the battlespace.

The WOC is the performance characteristic that can be used to gauge the probability of mission success and make wiser decisions regarding the employment of expensive agents to perform the search and attack function. One can readily assess the value of the objective and the probability that the objective will be successfully completed against the value of the munition. This usefulness is itself one of the most valuable outcomes of this research. Indeed, even modern day manned aircraft have a quantifiable sensor characterization (quantified by c). Thus, current manned flying operations could use this theory to obtain the probability of mission success without ever leaving the ground.

5.3 Concurrent Work in Simulation and Experimentation

Concurrent research at AFIT in the field regarded by this thesis produced satisfying corroboration in simulation and experimentation. The Air Force Research Lab (AFRL) maintains a high-fidelity UAV simulation named "Multi-UAV" that was used by Captain Michael Marlin in related thesis research [10]. One of the results that Capt Marlin produced was Monte Carlo simulations that duplicated the performance characteristic solved analytically in this work. The simulation was able to duplicate a stochastic battlespace defined by scenario 1. A munition of varying sensor ability (quantified by c) was flown in simulation against various numbers of false targets (quantified by λ_{FT}) and the statistical frequency of mission success (attack of the intended target) closely agreed with the probability determined by the theoretical algorithm in this thesis.

The other concurrent thesis that was accomplished during this time frame was an experimental validation of the concepts related to this thesis [11]. An experimental testbed was developed which entailed a remote-controlled car with a camera sensor. A car was chosen to simplify the problem from three dimensions to two. The car represented a UAV flying at a constant altitude. The camera was able to distinguish colors and a threshold of the number of pixels present in the field of view was established as the sensor threshold analog in this thesis. Different types of targets (i.e. true vs.

false targets) were created from different sized shapes of the color to which the sensor threshold was sensitive. The mock-munition was characterized by observing the frequency of correct vs. incorrect classifications at different sensor threshold levels. Essentially, each trial produced a separate confusion matrix. As mentioned in this thesis, every search system has an associated c; the value of c for the experimental car was identified by tuning the variable c in the ROC equation (equation 2.9) to produce the best fit ROC for the experimental sensor setup. The testbed established and described in [11] is a real-world, reproduction of the theoretical results proposed in this thesis and validated in simulation.

5.4 Recommendations for Future Work

There are ample opportunities for future research extending the results of this thesis. First, the optimal results from this theoretical work should be combined with the optimal decision rules developed in Gillen's and Dunkel's theses. The ultimate goal is to produce autonomous munitions that operate optimally by themselves and as part of a cooperative swarm.

In addition the experimental testbed begun by Capt Rufa should definitely be continued. There is a great deal of additional research that can be accomplished to the end of reproducing the actions of an autonomous munition, or even better yet multiple, cooperating, autonomous munitions. The theory developed in this thesis can be used to predict the performance of the experimental testbed. Evaluating the theoretical prediction and the experimental result in concert will inevitably shed substantial light on the utility of the practical application of this theory.

5.5 Conclusion

This thesis provides the justification for optimizing search and attack agent performance in a stochastic battlespace with false targets, and develops and solves the optimal control problem maximizing the performance of the agent. The mathematical foundation for the optimal control problem is sound and furthermore the

mathematical assumptions forming the foundation of this problem are not made in a vacuum. Readily available battlespace intelligence and present and foreseeable search and attack activities form the backbone and justification for the theory. With a reasonable estimate as to the expected number of false targets in the battlespace area, and a good characterization of the sensor/platform package one may confidently generate an expected probability that a given target will be attacked by an autonomous munition as well as the probability that any undesired objects might be attacked. The aggregation of the true target and corresponding false target probabilities forms the weapon operating characteristic, the performance metric for a search and attack munition in a stochastic battlespace with false targets.

Bibliography

1. Aurthur E. Bryson, Jr. *Dynamic Optimization.* Addison Wesley Longman, Inc., 1999.

2. Decker, Douglas D. *Decision Factors for Cooperative Multiple Warhead UAV Target Classification and Attack with Control Applications.* Doctoral dissertation, Air Force Institute of Technology (AU), Wright-Patterson AFB, OH, October 2004.

3. Dunkel, Robert E. *Investigation of Cooperative Behavior in Autonomous Wide Area Search Munitions.* Master's thesis, Air Force Institute of Technology (AU), Wright-Patterson AFB, OH, March 2002. AFIT/GAE/ENY/02-4.

4. Gillen, Daniel P. *Cooperative Behavior Schemes for Improving the Effectiveness of Autonomous Wide Area Search Munitions.* Master's thesis, Air Force Institute of Technology (AU), Wright-Patterson AFB, OH, March 2001. AFIT/GAE/ENY/01M-03.

5. Jacques, David R. and Robert Leblanc. "Effectiveness Analysis for Wide Area Search Munitions". American Institute of Aeronautics and Astronautics, Missile Sciences Conference, Monterey, CA, 1998.

6. Jacques, David R. and Meir Pachter. *Recent Developments in Cooperative Control and Optimization*, chapter A Theory of Cooperative Search, Classification, and Target Attack, 449–458. Kluwer Academic, 2004.

7. Kish, Brian A. *Establishment of a System Operating Characteristic for Autonomous Wide Area Search Vehicles.* Doctoral dissertation, Air Force Institute of Technology (AU), Wright-Patterson AFB, OH, September 2005.

8. Kish, Brian A., David R. Jacques, and Meir Pachter. "Search Operations Optimization". American Control Conference, 2005.

9. Kish, Brian A., David R. Jacques, and Meir Pachter. "Optimal Control of Sensor Threshold for Autonomous Wide Area Search Munitions". American Institute of Aeronautics and Astronautics, Guidance, Navigation, and Control Conference, San Francisco, CA, August 15-18, 2005. Paper 2005-6190.

10. Marlin, Michael J. *Wide Area Search and Engagement Simulation Validation.* Master's thesis, Air Force Institute of Technology (AU), Wright-Patterson AFB, OH, March 2007. AFIT/GAE/ENY/07-M17.

11. Rufa, Justin. *Experimental Development of Autonomous Wide Area Search and Engagement Applications Using Dynamic Scaling.* Master's thesis, Air Force Institute of Technology (AU), Wright-Patterson AFB, OH, March 2007. AFIT/GAE/ENY/07-M20.

Vita

Capt Rosario graduated from the U.S. Air Force Academy in 2002 with a B.S. in Aeronautical Engineering. His first assignment was at the National Air and Space Intelligence Center, Air Weapons Branch, WPAFB, OH. He completed the 18-month Master of Science program at AFIT in March 2007 with dual degrees in Aeronautical Engineering and Systems Engineering. After AFIT he proceeded to his next assignment with the 780th TS at Eglin AFB, FL.

Permanent address: 2950 Hobson Way
Air Force Institute of Technology
Wright-Patterson AFB, OH 45433

REPORT DOCUMENTATION PAGE

Form Approved
OMB No. 074-0188

1. REPORT DATE *(DD-MM-YYYY)*	**2. REPORT TYPE**	**3. DATES COVERED** *(From – To)*
22-03-2007	**Master's Thesis**	September 2005-March 2007

4. TITLE AND SUBTITLE

OPTIMAL SENSOR THRESHOLD CONTROL AND THE WEAPON OPERATING CHARACTERISTIC FOR AUTONOMOUS SEARCH AND ATTACK MUNITIONS

5a. CONTRACT NUMBER

5b. GRANT NUMBER

5c. PROGRAM ELEMENT NUMBER

6. AUTHOR(S)

Rosario, Roland A., Captain, USAF

5d. PROJECT NUMBER

5e. TASK NUMBER

5f. WORK UNIT NUMBER

7. PERFORMING ORGANIZATION NAMES(S) AND ADDRESS(S)

Air Force Institute of Technology
Graduate School of Engineering and Management (AFIT/EN)
2950 Hobson Way, Bldg 640
WPAFB OH 45433-7765 DSN: 785-3636

8. PERFORMING ORGANIZATION REPORT NUMBER

AFIT/GAE/ENG/07-02

9. SPONSORING/MONITORING AGENCY NAME(S) AND ADDRESS(ES)

AFRL/VA
Robert Murphey robert.murphy@wpafb.af.mil
2130 8th St.
Wright-Patterson AFB, OH 45433 MAJCOM: AFMC
(937) 255-6500

10. SPONSOR/MONITOR'S ACRONYM(S)

11. SPONSOR/MONITOR'S REPORT NUMBER(S)

12. DISTRIBUTION/AVAILABILITY STATEMENT

APPROVED FOR PUBLIC RELEASE; DISTRIBUTION UNLIMITED

13. SUPPLEMENTARY NOTES

14. ABSTRACT

This Thesis considers the optimal employment of a wide area search munition in a battlespace where a target is known to be uniformly distributed among false targets which are Poisson distributed. The Poisson distribution's parameter is obtained from readily available battlespace intelligence. This work formulates and solves the optimal control problem for deriving the optimal sensor threshold schedule in order to maximize the probability of attacking the target during the battlespace sweep while constraining the probability of attacking a false target. The efficiency gained by optimally varying the sensor threshold is compared against the performance achieved with a static, optimum sensor threshold setting. The Weapon Operating Character-
istic, the relationship between maximum achievable probability of target attack and maximum allowable probability of false target attack, is developed.

15. SUBJECT TERMS

Optimal control, autonomous, munition, search and attack, weapon operating characteristic

16. SECURITY CLASSIFICATION OF:			**17. LIMITATION OF ABSTRACT**	**18. NUMBER OF PAGES**	**19a. NAME OF RESPONSIBLE PERSON**
REPORT	**ABSTRACT**	**c. THIS PAGE**			**Meir Pachter, PhD (ENG)**
U	**U**	**U**	**UU**	77	**19b. TELEPHONE NUMBER** *(Include area code)* (937) 255-6565; email: meir.pachter@afit.edu